This is to certify that the

thesis entitled

Functional MRI of Cortical Activation During
Muscle Contraction and Fatigue

presented by

Robert W. Reid

has been accepted towards fulfillment
of the requirements for

Master's degree in Physiology

Major professor

Date 6/14/91

FUNCTIONAL MRI OF CORTICAL ACTIVATION DURING MUSCLE CONTRACTION AND FATIGUE

By

Robert W. Reid

A THESIS

Submitted to

Michigan State University

In partial fulfillment of the requirements

For the degree of

MASTER OF SCIENCE

Department of Physiology

2001

ABSTRACT

FUNCTIONAL MRI OF CORTICAL ACTIVATION DURING MUSCLE CONTRACTION AND FATIGUE

By

Robert W. Reid

The first part of this thesis examined the effect of the magnitude of muscle force on the intensity of functional Magnetic Resonance Imaging (fMRI) response in the primary motor cortex. An fMRI study was conducted with echo planar image acquisition using 13 volunteers who squeezed a custom built handgrip exerciser. Subjects performed isometric muscle contractions between periods of rest using 25%, 50% or MAX MVC. Regions of interest (ROI) were selected in the primary motor cortex and the mean signal intensity of the fMRI response was determined. The second part of the thesis investigated the effect of muscle fatigue on the fMRI response. Subjects were asked to perform 30-second bouts of MAX MVC, flanked by 30-second rest periods during eight and a half minutes of echo planar imaging.

There were two major findings of this study. First, the results show that there is a significant effect of isometric force on the fMRI response in the contralateral motor cortex. Second, the results provide no evidence that the fMRI response in the motor cortex is altered by muscle fatigue. However, further studies will be needed to demonstrate the generality of these results to other exercise and fatigue conditions.

TABLE OF CONTENTS

List of tables iv

List of figures v

Chapter 1: Background and Significance. 1
Introduction 1
Overview of the control of muscle activity and fatigue. 3
The basis of functional MRI. 7
Limitations of functional MRI 9
Other cortical activation measurement techniques 11
Functional MRI and motor activation 12

Chapter 2: Methods 15
Human subjects 15
Force measurements 15
Exercise protocols 18
MRI acquisition. 20
Data processing 21
Statistical considerations 28

Chapter 3: Results 29
Force Levels 29
Region of fMRI activation 32
FMRI response to each of the exercise conditions 36
Effects of fatigue on signal intensity 44

Chapter 4: Discussion and Future Directions 46

References 52

LIST of TABLE S

Table 1: Summary of raw force data 31

Table 2: Summary of raw voxel intensity data.....39

Table 3: Summary of motion corrected voxel intensity data 40

LIST of FIGURES

Figure 1: Summary of raw force data 6

Figure 2: Calibration curve of Weight (lbs) versus Voltage (v) 16

Figure 3: Sample WINDAQ display screen of muscle force output 17

Figure 4: Sample timeline of work/rest cycles 19

Figure 5: Anatomical 3DSPGR MRI image of the human brain 22

Figure 6: The time course of nine neighboring voxels in the axial plane 24

Figure 7: Region of Interest (ROI) of possible motor and sensory activation 25

Figure 8: Seven sample reference waves showing increased periods of activation and decreased rest periods 26

Figure 9: Example of reference wave fitted to a ROI is signal intensity time course 27

Figure 10: Raw force data recorded during the 25%, 50% and maximal MVC trials 30

Figure 11: Loss of force from the first two cycles to the last two cycles 33

Figure 12: Signal Intensity of voxels from the primary motor area versus time for 3 different force levels 34

Figure 13: Mean intensity of voxels from the primary motor area versus time for 100 % MVC 35

Figure 14: Motion corrected voxel intensity from the primary motor area for 3 exercise trials 37

Figure 15: Motion corrected signal intensity of voxels from the primary motor area during the maximal MVC trial 38

Figure 16: Bar graph showing percent change in voxel intensity in raw and motion corrected data 42

Figure 17: Simple linear regressions of individual subjects 43

Figure 18: Comparison of first 2 cycles to the last 2 cycles of the raw and motion corrected voxel intensity data 45

Chapter 1: Background and Significance.

Introduction

Functional MRI (fMRI) is a magnetic resonance imaging technique that exploits changes in tissue ^{1}H-NMR properties in order to measure a particular physiological response. By detecting changes in signal intensity of images of the brain, this modality can be used to monitor local changes in brain activity in real time (for a review, see Ogawa 1998). A number of studies have characterized the ability of fMRI to map the location of activity in the primary somatosensory and motor cortex during a variety of motor tasks. The overall aim of this thesis was to explore the use of fMRI for quantitative studies of the role of the central nervous system in the activation and maintenance of motor activity during submaximal and fatiguing isometric exercise.

The first aim of this thesis was to examine if there is a consistent relationship between the intensity of the fMRI response in the motor cortex versus muscle isometric force. It is well known that increased force of voluntary muscle contractions depends on recruitment of additional motor units, which in turn depends on increased synaptic input from cortical areas in the brain. Surprisingly, no published fMRI studies have unambiguously shown force-dependent changes in the intensity of cortical activity during muscle contraction. Two previous groups examined the effect of variations in the force of handgrip exercise on the fMRI response in human subjects. The first group, who used a dynamic weight-lifting exercise, found no effect of increased weight on the cortical response (Ludman, Cooper et al. 1996). The second group, who used an isometric exercise, reported increased *area* of fMRI activation, but only a small, statistically insignificant change in *intensity* of the fMRI response (Thickbroom, Phillips et al. 1998).

Resolution of this question is a necessary prerequisite for application of fMRI to the study of fatigue.

The second aim of this thesis was to examine if the fMRI response in the motor cortex is altered by muscle fatigue. It is generally accepted that two components can play a role in the fatigue of muscle during exercise (Bigland-Ritchie and Woods 1984): peripheral and central. Peripheral fatigue refers to decreased force generation in the muscle fibers themselves, and is sometimes referred to as "muscle contractile failure" (Porter 1981). Although not completely understood (see Fitts 1994 for a comprehensive review of the cellular mechanisms of peripheral fatigue), this component is thought to result from local accumulation of metabolites such as inorganic phosphate, drops in pH, and/or depletion of ATP supply. In contrast, central fatigue is a decline in force due to the central nervous system failing to maintain muscle activation or "central drive" (Bigland-Ritchie and Woods 1984). Whether central or peripheral components are dominant likely depends on the exact nature of the exercise. For example, during relatively prolonged exercises decreased central drive may be the dominant factor (Bellemare 1984, Bigland-Ritchie and Woods 1984, see below). In that case, assuming that the fMRI response in the motor cortex is related to the intensity of cortical activation, one might expect decreased fMRI response during fatigue. On the other hand, during very intense, repetitive voluntary exercise, when peripheral factors are likely to be dominant, central drive might increase, as the subject attempts to maintain the target force. In that case, one might expect the cortical fMRI response to increase during fatigue. Of course, because there is at present no widely accepted measure of central

drive, it is difficult to predict a priori the likely result for any particular exercise protocol. Therefore, the results of this study are only a first step in addressing these issues.

Overview of the control of muscle activity and fatigue.

Before any intended muscle movement can occur, neural commands from higher centers must translate neural information into the intended actions. Intent to perform a motor task begins in the higher centers of the brain with the initial activity taking place in frontal lobe regions of the cortex (Deecke, Scheid et al. 1969, Ghez 1991, Thickbroom, Byrnes et al. 2000). In close association with frontal cortex activity is the activation of the premotor area, which in turn activates anatomically specific motor areas in the primary motor cortex corresponding to the desired motor function (Ghez 1991), Thickbroom, Byrnes et al. 2000). However, many regions throughout the brain are involved in the processing to ensure that the executed motor activation matches the intended behavior. For example, inhibition via the motor circuit of the basal ganglia must be removed to allow for stimulation of the premotor cortex (Cote 1991). The cerebellum plays a key role, receiving input pertaining to the desired motor function from the cortex, while concurrently receiving feedback from the spinal cord and periphery about the evolving muscle movement (Ghez 1991). The spinocerebellum processes the incoming information to finely tune the motor activity into a fluid motion allowing proper muscle forces to maintain the desired behavior. From the primary motor area (Brodman's area 4), the descending corticospinal tract provides a direct pathway for muscle activation by travelling down the contralateral side until reaching a level of the spinal cord, where primary motor neurons synapse onto lower motor neurons and interneurons (Kelly 1991). Lower motor axons then travel out of the ventral roots of the spinal column to the

muscles of interest. The lower motor axons act on muscle fibers by releasing acetylcholine at the motor end plates, leading to excitation coupling and contraction of the motor unit. In addition, muscle spindles and other sensory organs provide feedback to both spinal and supraspinal areas. All of these components must be working correctly with the overall result being a motor movement that matches the intended behavior.

Given the complexity of motor control, it is not surprising that our understanding of central factors in muscle fatigue is limited. In a review by Enoka and Stuart (Enoka and Stuart 1992), muscle fatigue was defined as a general concept intended to denote an acute impairment of performance that includes both an increase in the perceived effort necessary to exert a desired force and an eventual inability to produce this force. How fatigue occurs depends on a number of factors including the strategy of both agonist and antagonist muscle recruitment, the speed and force of the individual muscle contractions, and the intensity and duration of the overall activity (Enoka and Stuart, 1992).

It is relatively easy to demonstrate that peripheral factors play the major role in fatigue during very intense exercises. For example, major drops in muscle force output can be induced by direct electrical stimulation of isolated muscles, where central factors could play no role (Adams et al. 1991, Fitts 1994). Although the exact mechanism of fatigue under these conditions is not understood, there is a good correlation between metabolic events (e.g., inorganic phosphate accumulation, decreased pH) and the decline in force. Because very similar force and metabolite changes are observed in muscles of human subjects during intense, repetitive voluntary exercise (Cady et al. 1989), it is generally assumed that peripheral, metabolic factors are largely responsible for fatigue under those conditions.

Nonetheless, some studies using the twitch-interpolation method suggest that decreased central drive plays some role in fatigue even during intense voluntary exercise (Bigland-Ritchie et al. 1986, Mckenzie et al. 1992). In this method (Merton 1954, Hales and Gandevia 1988), central drive is estimated from the mechanical response to administration of an electrical stimulus to the muscle during a maximal voluntary effort. If the stimulus results in increased force above the voluntary force, it is assumed that some motor units were not activated by the effort. During fatigue, the relative size of the interpolated twitch increases, suggesting decreased central drive.

During low intensity, long duration exercise, central factors may be more important, inasmuch as there is little evidence for peripheral metabolic fatigue under these conditions. Bigland-Ritchie and Woods have emphasized that the time for which an exercise can be performed is inversely dependent on the intensity of the exercise (Figure 1). They suggest that central fatigue becomes increasingly dominant as the intensity of the exercise decreases and the duration increases. If this suggestion is correct, then the exact choice of exercise intensity and duration could profoundly alter the results of a study such as this one. Again however, there is little direct evidence for this suggestion, and in any case there are few previous studies upon which to base the choice of exercise protocol for this study.

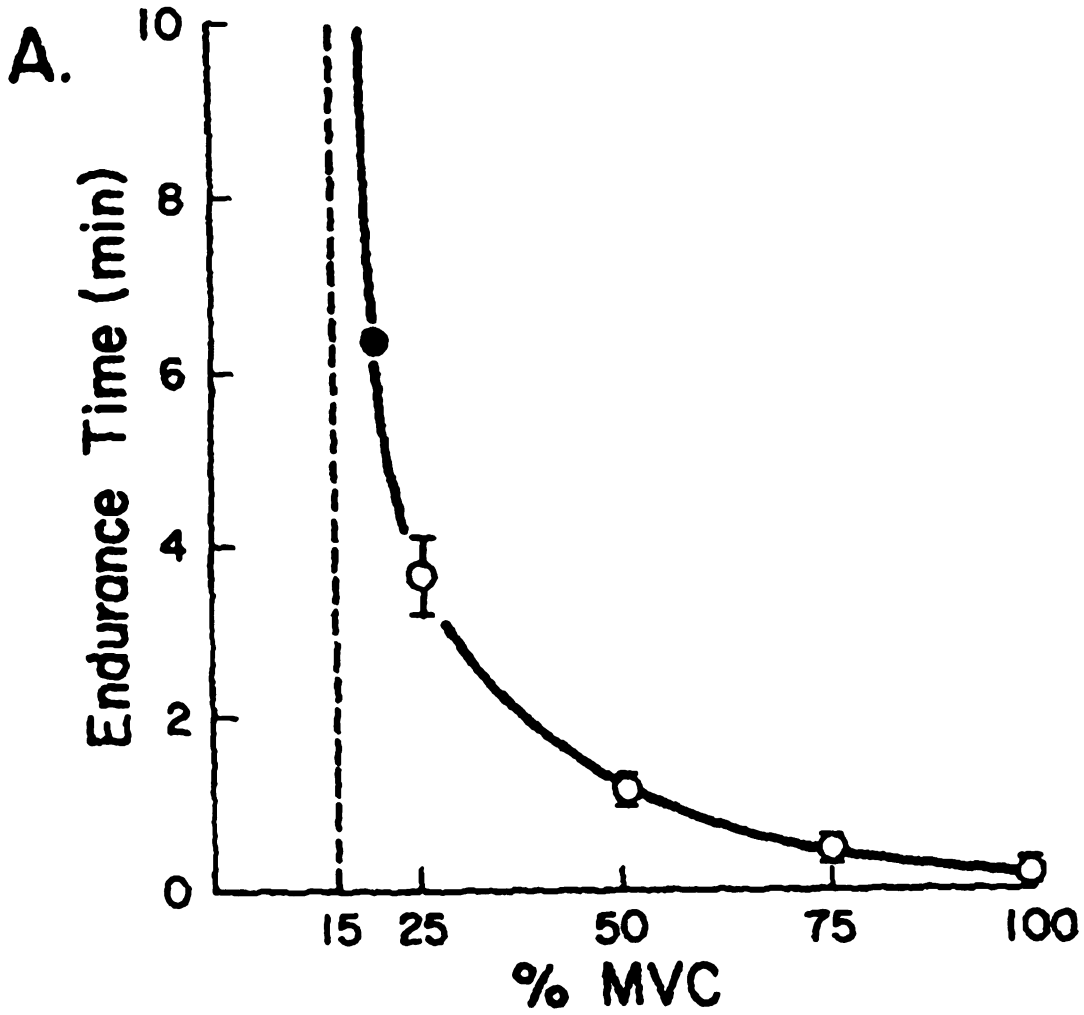

Figure 1: Graph of percent of maximal voluntary contraction (% MVC) versus duration of muscle contraction

The amount of time that the %MVC can be maintained before muscle failure occurs. For any %MVC below 15%, muscle failure does not occur. (Bigland-Ritchie and Woods 1984)

The basis of functional MRI.

Active brain cells require chemical energy in the form of ATP for the energy dependant processes of ion homeostasis, neurotransmitter synthesis, and synaptic vesicle formation (Schwartz 1991). Furthermore, glial cells near active neurons also degrade neurotransmitters and aid in ion homeostastis, and therefore also increase their rate of metabolism. This increased energy demand during neural activation is directly coupled to increased local blood flow (Gyngell, Bock et al. 1996, Raichle, Grubb et al. 1976, Olesen 1971, Ogawa, Menon et al. 1998, Roland 1980). The regulation of local brain blood flow is not fully understood, but is thought to depend on factors such as increased extracellular K^+, decreased cellular PO_2, decreased local pH, and cellular adenosine release (Ganong 1991). This brings about an increase in permeability in the tight junction of endothelial cells (Rapoport 1976) and localized vasodilation. As O_2 and CO_2 easily pass across the blood brain barrier, a transient increase in blood flow (Grubb, Raichle et al. 1974) allows O_2 and CO_2 transfer, which support the metabolic needs of the brain. Direct evidence of regional increases in brain blood flow were demonstrated over two decades ago by monitoring increases in regional cerebral blood flow (rCBF) via 133Xe clearance (Roland and Larsen 1976) during periods of increased neural activity (Raichle, Grubb et al. 1976), (Olesen 1971), (Roland, Larsen et al. 1980).

It is possible to measure local brain perfusion using MRI methods, and some fMRI studies are based on direct flow measurements. However, most brain fMRI studies are based on a related phenomenon known as the BOLD (blood-oxygenation-level-dependent) effect (Ogawa, Lee et al. 1990, Bandettini, Wong et al. 1992, Ogawa, Menon et al. 1993). This phenomenon depends on the effect of oxygen on the magnetic

properties of blood. Specifically, the magnetism of the iron atom in hemoglobin is stronger when the hemoglobin is deoxygenated compared to when it is oxygenated. Therefore, deoxygenated blood has a higher magnetic susceptibility, and causes greater distortion of an applied magnetic field than does oxygenated blood. Distortions of the magnetic field around blood vessels enhance the transverse relaxation rates (1/T2 and 1/T2*) of the surrounding tissue, and therefore, decrease the signal intensity in T2- and T2*-weighted MR images. (Ogawa, Lee et al. 1990). T_2 is the time constant that characterizes the intrinsic rate of decay of transverse phase coherence after an initial excitation of nuclei in a static magnetic field (Farrar 1971), (Shaw 1976) (Hornak 2000). The T_2^* time constant is the combined effect of T_2 and the additional phase dispersion due to static field distortions (Ellerman 1994). Both T_2 and T_2^* relaxation are exponential processes, and changes in both can occur via changes in deoxyhemoglobin content, resulting in changes in MRI signal intensity.

Surprisingly, it has been shown that blood flow increases more than local oxygen consumption in active regions of the brain (Fox, Raichle et al. 1986). Therefore, PO2 increases in active regions, blood becomes more oxygenated, and local MRI signal intensity increases in the active regions. At the field strength of clinical imagers (1.5 Tesla) the effect is small (a few percent signal change) but can be reliably measured, especially if many scans are acquired, so statistical tests with good power can be performed. The vast majority of fMRI studies are based on measurement of these BOLD-based changes in MRI signal intensity.

Limitations of Functional MRI

Unfortunately, there are several limitations to fMRI. First, because the underlying NMR signal is relatively weak, the spatial resolution of MRI is relatively low. This is particularly a problem in fMRI studies, in which good time resolution is also needed. The voxel size of fMRI images acquired at 1.5 T typically ranges from 30 to 100 mm^3. Therefore, even the smallest fMRI voxel includes hundreds or thousands of neurons, which may serve many different functions. Furthermore, some minimum but unknown fraction of the neurons within a specific region may need to change activity in order to induce a significant, detectable blood flow change.

A related problem is that small changes in neural activation may not be detected because they are lost amongst the normal variations in activity and signal intensity. The "basal" state may include a great deal of excitatory and inhibitory neuronal activity, as evidenced by the fact that the "resting" brain has a high metabolic rate and oxygen requirement (Brust 1991). In order to detect "activation", the change in signal must be large enough to alter the signal above this resting brain activity. Comparing one resting region to another is not a valid possibility because blood vessel density, tissue composition, and basal activity might be different in different regions. Therefore, experimental design for fMRI is constrained to comparisons of resting signal intensity vs. intensity acquired during a specified task.

A second general limitation of fMRI arises from the fact that it does not directly measure electrical activity, but instead measures a complex metabolic result of the activity. This has two consequences. First, because the BOLD effect depends on hemoglobin oxygenation, the effect can be saturated. Therefore, there is no assurance that

the signal changes depend linearly on local neuron activity (Bandettini, Wong et al. 1992). Second, there may be a time delay of up to 5 to 6 seconds between the activation of neurons and the maximal BOLD response. Even when detection of the hemodynamic response is rapid, the image acquisition will still be separated temporally from the actual neural events (Ellerman 1994). An investigator needs to be cautious when examining BOLD response changes as the temporal limitation could vary in different areas of the brain over short time courses (Blamire, Ogawa et al. 1992), (Ellerman 1994). Detection of activation in one brain region before another region may not necessarily mean that both regions were not activated at the same time. This limitation of fMRI must be considered when looking at the rate at which a region becomes active. Furthermore, in studies aimed at relating the intensity of the fMRI response to another parameter such as force, the task duration must be sufficient for the hemodynamic response to fully develop. Similarly, if the study includes "rest" periods between the tasks, these must be of sufficient duration for the response to decay back to baseline.

A third limitation to fMRI is motion artifacts. Over time, some degree of motion inevitably occurs. Head translation in normal resting subjects has shown to be less than 1 degree of rotation over an hour (Zeffiro 1996), but even this slight deviation is sufficient to cause image artifacts. Because the BOLD signal is only a few percent change, even a small displacement of the image voxels across regions with different intensity can have very large effects. If the motion occurs in synchrony with the task under study, these motion induced-changes will mimic task-related activation. Therefore, to maximize the accuracy of fMRI, head motion needs to be kept to an absolute minimum.

Finally, other imaging artifacts can complicate fMRI interpretation. For example, the echo-planar imaging method commonly used in fMRI studies is particularly sensitive to magnetic susceptibility artifacts around bones and air-filled sinuses (Savoy 2001). These artifacts can severely distort or even eliminate signal from adjacent brain regions. Similarly, variations in coil tuning, magnet homogeneity, and other instrument settings alter the absolute signal intensity, making direct comparisons between subjects difficult.

Other cortical activation measurement techniques

Detection of cortical activity changes via MRI shows good correlation with other metabolic brain measurement techniques such as Positron Emission Tomography or PET (Ramsey, Kirkby et al. 1996). Both techniques are able to show specific regional activation in the cortex during an applied stimulus. PET scans have the disadvantage of requiring injection of a tracer whereas fMRI is completely noninvasive (Martin 1991). Another technique that is increasingly used for investigating brain motor function is transcranial magnetic stimulation or TMS (Rothwell 1997, Ilmoniemi, Ruohonen et al. 1999, Chen 2000). TMS passes a current through a wire coil placed on the scalp. A large changing magnetic field induces current in the underlying brain to cause stimulation and manipulation of cortical activity (Ilmoniemi, Ruohonen et al. 1999, Chen 2000). This technique can be combined with anatomical MRI to determine where the stimulation actually occurs. This technique is painless unlike the traditional electrical stimulation (TES) as performed by Merton in the early eighties (Merton and Morton 1980). Functional MRI can monitor changes in the cortex but it does not provide means to create cortical stimulation like TMS can. Combined, these two techniques would make a powerful investigative tool and attempts have been made to use the two techniques in

concert (Ilmoniemi, Ruohonen et al. 1999). Unfortunately, TMS is not yet widely available.

Functional MRI and motor activation

The use of fMRI as a tool for studying motor activity has focused primarily on mapping of the motor cortex. Bandettini et al. (Bandettini, Wong et al. 1992) were among the first to use fMRI to demonstrate that changes in intensity in the primary motor area correlated with a motor task. Further studies mapped both the primary sensory (Roberts and Rowley 1997) and motor areas (Yetkin, Mueller et al. 1995, Boroojerdi, Foltys et al. 1999, Kim, Ashe et al. 1993, Rao et al. 1993). More recent studies have focused on mapping regions involved in motor planning, including studies of fairly complex motor tasks (Thickbroom, Byrnes et al. 2000, Koechlin, Corrado et al. 2000). Mapping of the motor cortex using fMRI could be of clinical use as a possible diagnostic tool before brain surgery, and accordingly much of the current work is focusing on adaptations to stroke and other pathologies.

Although use of fMRI to characterize the location of neural activation during a motor task has been well documented, little attention has been paid to the intensity of the activation. Thus far, only three papers have attempted to investigate what happens to the intensity of the motor fMRI response during muscle contractions. The first was the study by Ludman et al. (Ludman, Cooper et al. 1996) that used a dynamic finger flexion weight-lifting exercise with heavy vs. light weights. This study found that a five-fold increase in weight lifted had no effect on the intensity of the fMRI response in the sensorimotor cortex. However, this study is not conclusive, because the use of a dynamic exercise to investigate the fMRI response adds a major tactile and proprioceptive

component, which could cause a similar pattern in the fMRI response regardless of the force of muscle contraction (Thickbroom et al. 1999).

In the second paper investigating the effect of force on signal intensity, Thickbroom et al. (Thickbroom, Phillips et al. 1998) measured the fMRI response to a series of isometric handgrip exercises at different force levels. They found that an increase in the total cortical area occurred with increases in muscle force, but did not find a significant increase in signal intensity. In this study, the highest level of force used was 50% MVC, which may not be a sufficient force to illicit the maximum change in voxel intensity. Also, subjects were required to use four fingers to squeeze a modified sphygmomanometer bladder attached to a mercury column. This type of exercise could exclude activation from the thumb at lower levels of MVC, but at 50% MVC, subjects may have used their thumb muscles to increase stabilization. If this were so, then the observed increase in total cortical area of activation is not surprising, because the thumb has a relatively large representation in the motor homunculus. Furthermore, as subjects squeezed the bladder, they were required to watch the mercury column to maintain a constant level of force. A possible downside to this type of exercise protocol is that cognitive effort would be required to interpret and constantly correct the level of force. This cognitive effort could possibly mask any detectable fMRI changes due to muscle force per se. As noted below, we removed the feedback component of the exercise, and instead had each subject practice reaching the target force prior to the fMRI imaging session. Finally, the use of a fluid filled bladder device has another drawback. The initial squeezing of such a device could be dynamic in nature and require finger flexion up to the point where sufficient resistance occurs. In fact, in their more recent paper,

Thickbroom et al. found that the force and frequency of dynamic muscle contractions did not correlate with the fMRI response, but the dynamic exercise had a more pronounced effect on fMRI response than isometric exercises of similar force (Thickbroom, Phillips et al. 1999). Therefore, it may be that isometric exercise is more appropriate for studies of the effect of force on cortical fMRI signal intensity. For example, a previous PET study did find force-correlated changes in blood flow during isometric exercise (Dettmers 1995).

Based on the results of these previous studies, it appears that the relationship between the intensity of the fMRI response vs. force has not been clearly established. Therefore, the first aim of the following experiments was to examine if variations in isometric force alter fMRI intensity in the motor cortex. In addition, we began the exploration of the possible effect of fatigue on the fMRI response.

Chapter 2: Methods

Human Subjects

Thirteen subjects (age 18 to 30 years, 5 female) were recruited from the academic community. The study was approved by the University Committee on Research Involving Human Subjects, and subjects were informed about the purpose and procedures of the experimental protocol and gave written consent prior to participation. Subjects lay prone in the magnet throughout the experiments. Due to the confining nature of the imaging device, subject applicants who reported previous claustrophobic episodes were excluded from the study.

Force Measurements

The force of isometric handgrip contractions was measured using a custom-built strain gauge transducer device. This device consisted of a commercial plastic handgrip exerciser, fitted with a $1/4^{th}$-inch thick aluminum bar to which two semiconductor strain gauges where glued (Omega Engineering Inc., model 213.19-2004, 120 ohms, Stamford, CT). The gauges were arranged in a Wheatstone bridge, and bridge excitation and signal amplification were provided by a Gould transducer amplifier. The device was calibrated with weights, and its output was linearly dependent on weight in the range from 2 to 16 pounds (Figure 2). The calibration was checked prior to each new study by hanging a known weight of 2.23 Kg (10 lbs.) from the end of the hand grip and adjusting the amplifier gain to 1 volt output. During the experiments force was digitally recorded at 120 samples/s on a MS Windows 98 PC using a 12 bit A/D converter and serial data acquisition system

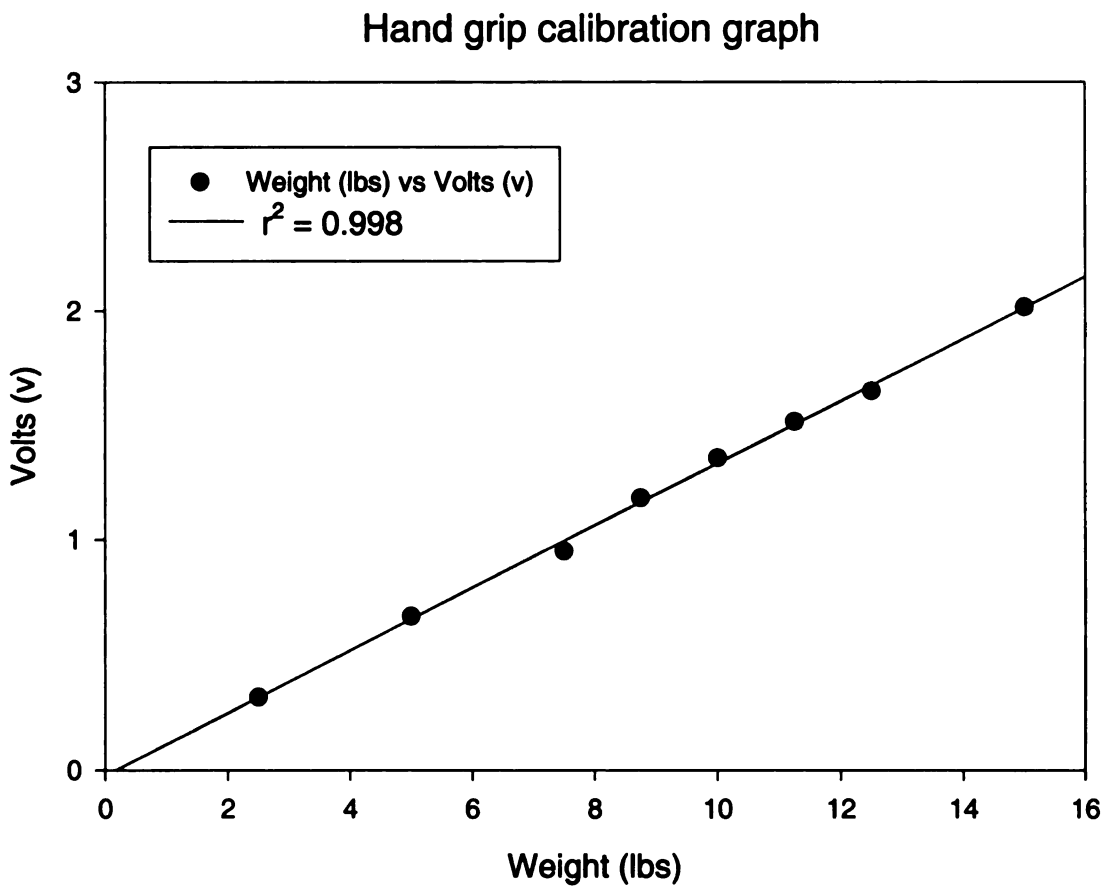

Figure 2: Calibration curve of Weight (lbs) versus Voltage (v)

Weights were added in random order to ensure that the handgrip device returns to starting position and that hysteresis is not occurring. Measurements were repeated 3 times.

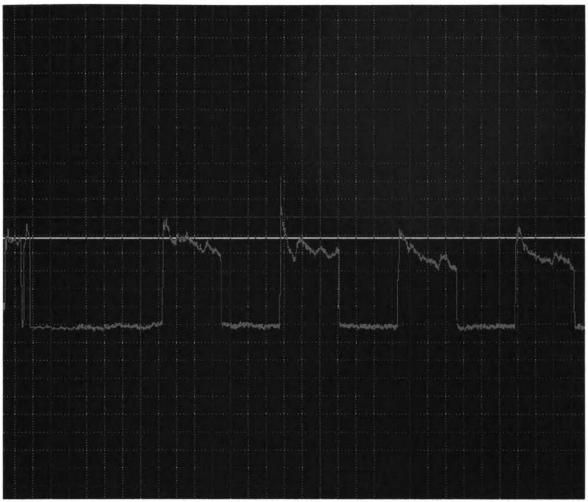

Figure 3: Sample WINDAQ display screen of muscle force output (DATAQ Instruments, Akron, OH)

The green line represents the amount of actual force being produced when squeezing the handgrip dynamometer. The yellow line represents the target level that subjects practiced trying to attain during each practice session prior to each imaging session. The above figure is on color.

(DATAQ Instruments, Model DI-151RS, Akron, OH). When appropriate (see below) a real-time display of force output was presented to the subject in the magnet on a 640x480 pixel LCD (IFIS MRI display system, MRI Devices Corporation, Waukesha, WI) using WINDAQ Lite software (DATAQ Instruments, see Figure 3).

Exercise protocols

The force of maximum voluntary contraction (MVC) was measured for each subject at the start of each study. MVC was measured as the mean of the peak force during the best two of 3-6 test contractions, each 5-10 seconds in duration, and recorded while the subject lay prone in the same position as during the MRI acquisitions. Based on the MVC measurement, forces corresponding to 25% and 50% MVC for each subject were computed. The subject then performed three exercise protocols, during which fMRI (see below) and force data was continuously acquired: 25%, 50%, and MAX exercises. The 25% and 50% exercises each consisted of four 30 s duration isometric contractions at that force level, separated and flanked by seven 30 s rest periods (4.5 min total duration, see Figure 4A). Prior to the 25% and 50% exercises the subject was allowed to practice achieving the target force by viewing the force record, along with a yellow trace corresponding to the target force, on the IFIS display (Figure 3). However, in order to simplify the motor task, force was not displayed to the subject during the experimental runs. Instead, the subjects were instructed to focus their attention on minimizing head motion (see below), and to contract only during the 30 s "WORK" phase of an alternating "REST"-"WORK" cue presented on the IFIS display. The 25% and 50% exercises were performed in random order, followed by the MAX exercise. The MAX exercise consisted of eight 30 s duration contractions, flanked by nine 30 s rest periods (8.5 min, see Figure

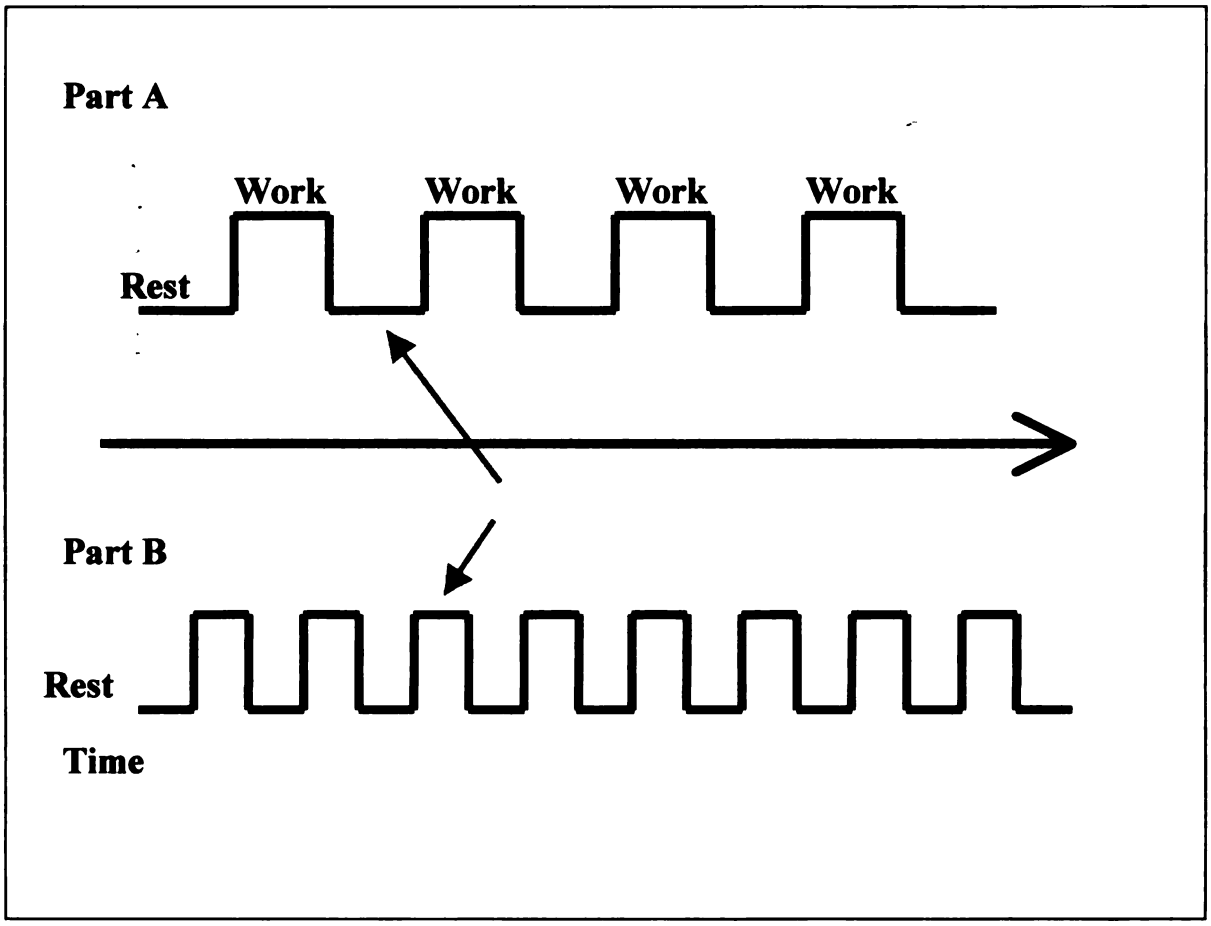

Figure 4: Sample timeline of work/rest cycles during the 25%, 50% and 100% MVC protocols

Part A represents the reference waveform for 25 and 50% MVC. Part B represents the protocol for MAX MVC, which involved 8 cycles of work/rest rather than 4 cycles. The above figure is on color.

4B). Prior to this run, the subjects were instructed to contract with maximum force during each "WORK" cue, but no practice contractions were performed. Subjects were instructed to contract "as hard as you can", consistent with maintaining head stability. Subjects were warned that this was likely to result in fatigue, but that they should continue to contract as hard as possible through the 8th contraction, unless unable to continue because of pain or discomfort. All subjects were able to complete the 8th contraction cycle.

Prior to each exercise the subjects were cautioned to avoid head motion. In order to aid the subjects in this task, we adopted the visual motion-sensing method described by Thulborn et al. (Thulborn 1999). A black string was taped horizontally across the subject's field of view halfway between the subject and the IFIS display screen. A reference line was then positioned on the IFIS display so that it was aligned with the string from the subject's perspective. Small motions of the head were then readily apparent to the subject from the displacement of the string relative to the reference line.

MRI acquistion

MR images were acquired on a GE 1.5 Tesla clinical scanner (Horizon ver. 8.4, GE Medical Systems, Milwaukee, WI) using a standard clinical bird-cage head coil. After subjects were comfortably positioned, landmarked and moved into the magnet, a T1-weighted saggital localizer scan was acquired (spin echo, minimum TE, TR= 500 ms, twenty 5 mm slices separated by 5 mm, 24 cm field-of-view, 256x160 acquisition matrix, 2 min total acquisition time). A high resolution anatomical 3D volume image of the entire brain region was then acquired while the subject was at rest (spoiled gradient-recalled echo, minimum TE and TR, 30 degree flip angle, 24 cm field of view, 1.5 mm

slice thickness, 124 slices, 256x128 acquisition matrix, 7 min total acquisition time). Functional images were then continuously acquired during each of the above three exercise protocols. The functional images were axial, one-shot, gradient-echo, echo-planar images with TR=3 s, TE=45 ms, 90 degree flip angle, 7 mm slice thickness with 1.5 mm separation, 20 slices, 24 cm field-of-view, and 64x64 acquisition matrix. A total of 1800 and 3400 images, or 90 and 170 images per slice, were acquired during the 25-50% and MAX exercise protocols, respectively. After each experimental session, both force and image data were transferred via the internet to a Sun workstation for later processing.

Data processing

Analysis of the fMRI data was performed in two steps: region-of-interest (ROI) selection and motion correction, followed by fitting of an idealized waveform to the ROI intensity variations. The ROI selection and motion correction was performed using the AFNI software package written and distributed by Dr. Robert Cox (Cox 1996, http://afni.nimh.nih.gov/afni). This is a general fMRI analysis package that includes software for display of anatomical and functional data sets, various statistical functions (e.g., cross-correlation, F-tests, multiple regression models), 2D and 3D motion correction algorithms, Talairach transformation, and overlay of functional and anatomic images (e.g. Figure 5). In each subject, an activated ROI was selected in the contralateral (typically left) sensory-motor area. Activated voxels were identified by cross-correlation against a smoothed on-off reference wave corresponding to the rest-work periods depicted in Figure 4. The AFNI deconvolution plug-in was also used to determine if and

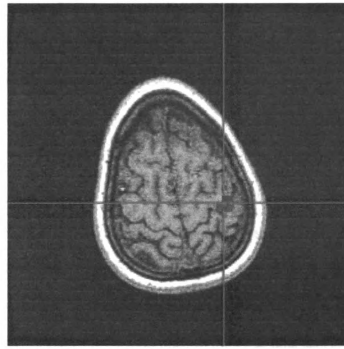

A

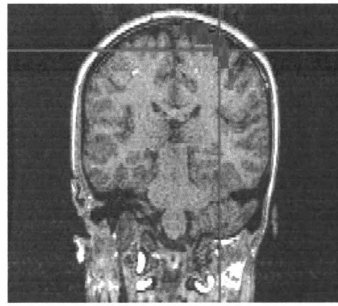

B

Figure 5: Anatomical 3DSPGR MRI image of the human brain

Panel A represents the axial plane. Panel B represents the coronal plane. The color overlay represents functional regions that correlate with the reference wave. The above figure is on color.

where statistical changes from resting conditions had occurred. The plug-in compares each voxel to the reference wave and determines if a significant change from the resting baseline has occurred during the on periods. Voxels demonstrating a high statistical difference ($p<0.001$) were considered for inclusion in the ROI. An example of the signal changes in single voxels appears in Figure 6. A contiguous subset of these voxels (mean number = 13.7 ± 2.3 (SE)) which were judged to be within or near the precentral motor area was then selected as the ROI for that that subject (see figure 7). This selection was made on the data from the first exercise protocol (i.e., randomly on the 25% or 50% exercise data). The same ROI was then applied to the other two data sets from the same subject. In addition, the same ROI was applied to the three data sets after motion correction using the 3D AFNI plugin. After ROI selection, the averaged time course of the signal intensity in the selected voxels was saved for further analysis.

To determine the relative increase in signal intensity in an unbiased manner, the ROI intensity-time data was fit to a series of 7 basic reference waveforms (Figure 8). These waveforms differed in the width of the "on" phase, in order to account for the fact that in many cases the hemodynamic response persisted well beyond the 30 s contraction duration (e.g., Figure 9). The fit was performed by linear correlation of the reference waves vs. the actual data. The intercept of this correlation yields the fitted baseline intensity, and the slope yields the mean change in intensity from baseline during the on periods:

$$Yi = \text{Slope} * Xi + \text{baseline},$$

where Yi is the intensity of the i^{th} datum point, and Xi is the intensity of the corresponding point in the reference wave. The percent change in intensity is then

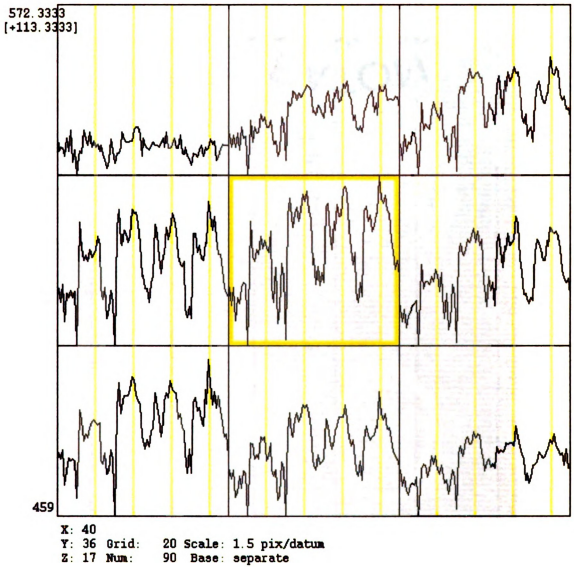

Figure 6: The time course of nine neighboring voxels in the axial plane

The above figure represents 9 individual graphs of 9 neighboring voxels within the primary motor cortex during an image acquisition of alternating exercise and rest periods. Each square represents a time series for one voxel. All neighboring voxels appear around the highlighted center voxel. The center voxel shows a pattern similar to the reference waves from Figure 4A, while the voxel in the upper left panel shows little similarity. The above figure is on color.

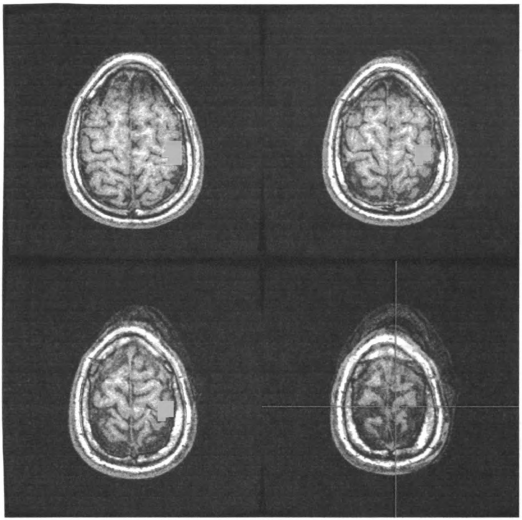

Figure 7: Region of Interest (ROI) of possible motor and sensory activation.

Yellow area represents the ROI. The ROI is laid over the region of activation. The above figure is on color.

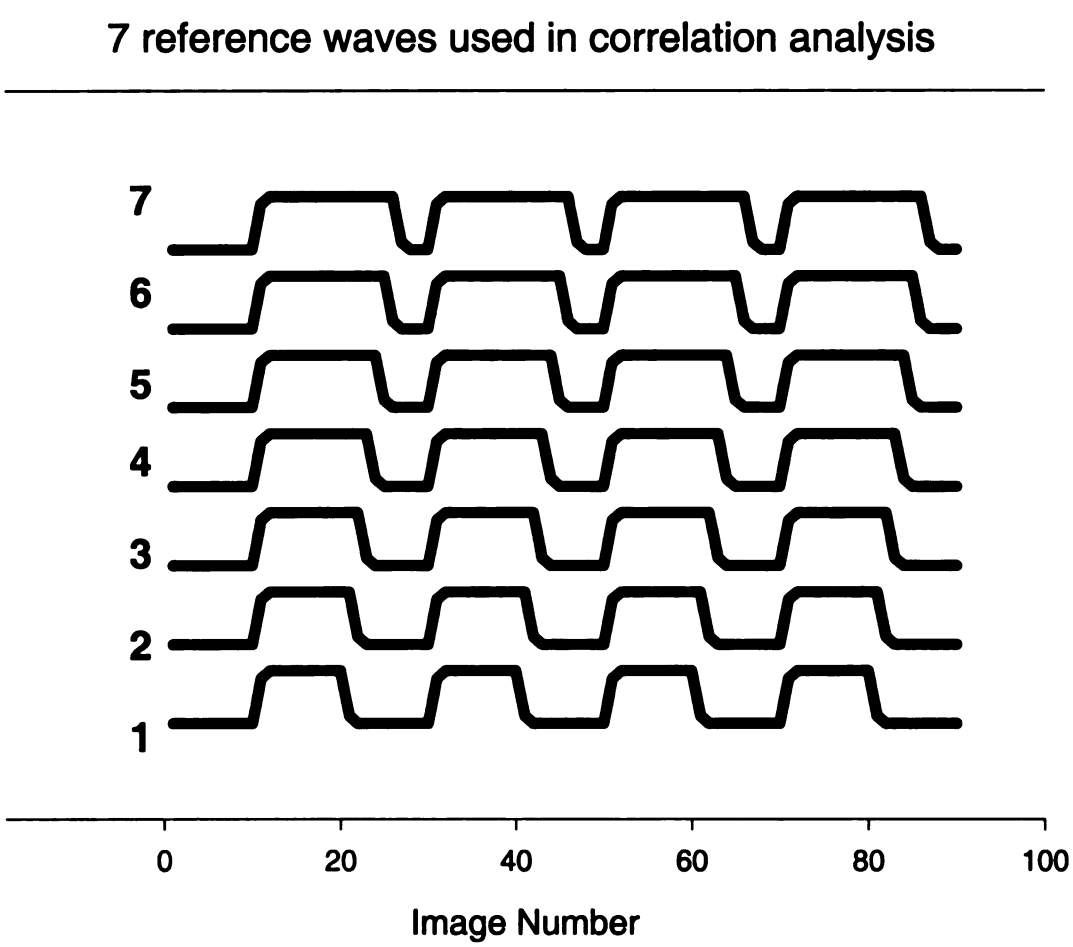

Figure 8: Seven sample reference waves showing increased periods of activation and decreased rest periods

The bottom most reference wave follows the same time course as the reference wave from figure 4A. Progressing upwards, each reference wave adds one image time point to the "WORK" cycle and removes one image data point from the "REST" cycle. A hemodynamic delay is also added to the wave forms

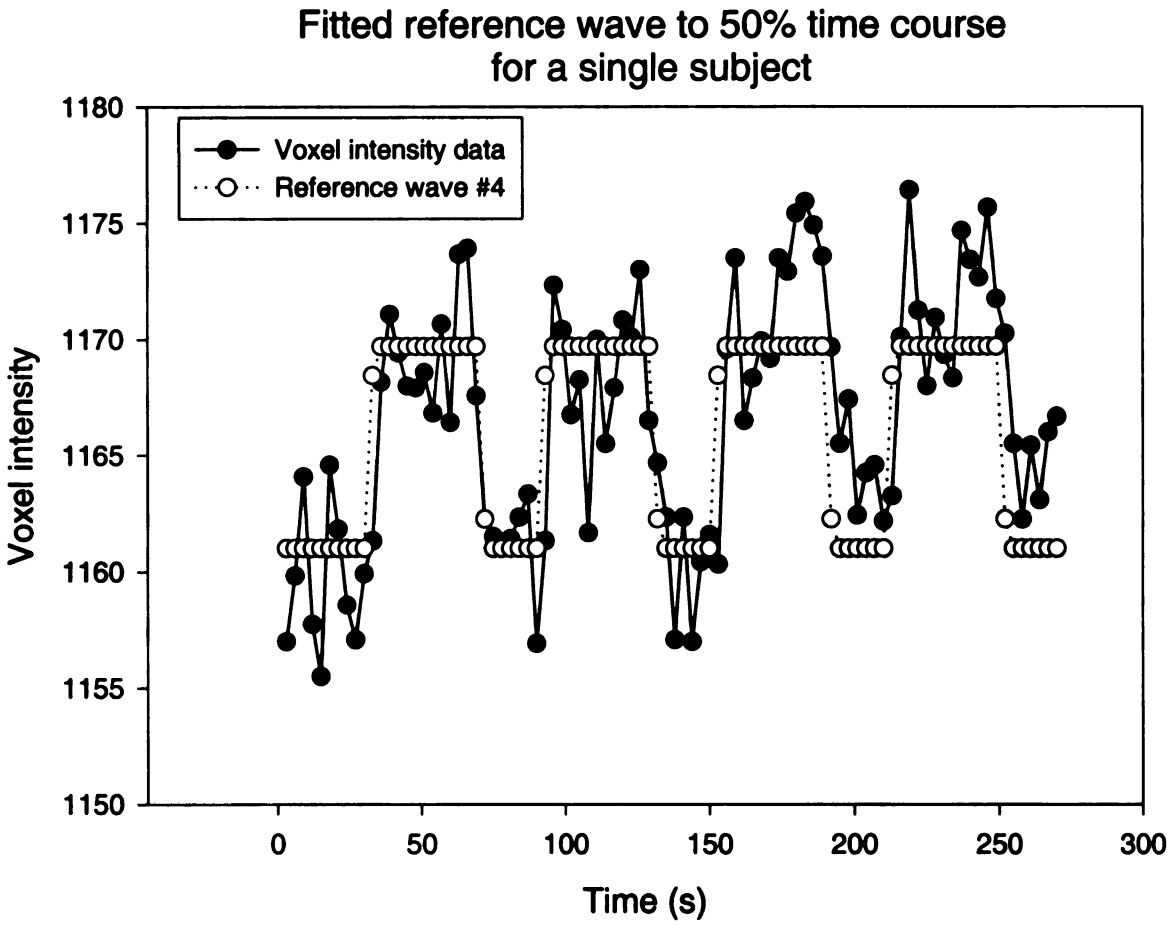

Figure 9: Example of reference wave fitted to a ROI is signal intensity time course

For this subject, the reference wave consisted of 7 "resting" data points and 13 "active" data points. A shift of 1has been applied in the right direction.

computed as (100* slope/baseline). This correlation was computed for the seven basic reference waves, and for the same basic waves shifted by up to 7 points in either direction (i.e., total of 105 trials). The best fit was the variation with the best correlation coefficient.

The MAX exercise data were analyzed in two ways. First, the first 4 rest-contraction cycles were analyzed exactly as the 25% and 50% exercises, using the reference waves in Figure 8. In addition, to determine if muscle fatigue affects the fMRI response, the average intensity of first two work cycles of the maximal MVC trial were compared to the signal intensities of the final two work cycles. This computation was performed as above, but using truncated versions of the 7 basic reference waves. Finally, this same analysis program was applied to the muscle force records to determine the average resting force levels and the average force during the contractions.

Statistical considerations

One way ANOVA, paired Student's t-tests, and Leven's test of homogeneity of variance were used to compare percent change in ROI intensity between the 3 different conditions using SPSS statistical software (SPSS, Inc.). After ANOVA, Tukey range tests were performed to determine which if any conditions differed from each other.

Chapter 3: Results

All 13 subjects succeeded in performing the 3 exercise tasks. Subjects often reported hand soreness, which is consistent with the development of localized muscle fatigue. Of the 13 subjects, 12 were right-handed and one left-handed. ROI analysis for the left handed subject was performed on the contralateral motor cortex, i.e., the right side of the brain. However, the left-handed subject along with two other subjects, were eventually excluded from the final data analysis because of excessive head-motion. Two additional subjects were removed from the final analysis because no detectable fMRI response was found when examining the AFNI functional-anatomical overlay.

Force Levels

The mean MVC for the eight subjects was 14.3±2.2 kg. Mean force recordings (n=8) during the 25%, 50% and MAX trials are depicted in Figure 10. Contrary to the instructions given to the subjects, force was not constant during the 30 s contractions. Instead, a peak in force occurred at all three levels of force during the initial part of the contractions. This phenomenon was more pronounced in the 50% and MAX exercises than in the 25% exercise. The average decline from the peak force in the 25%, 50% and MAX contractions was 19%, 28% and 26%, respectively. In order to obtain an unbiased estimate of the mean force during these contractions, we applied the correlation program described in Chapter 2 (see Table 1). Based on that analysis, the mean force during these exercises was 19.9±2.0 (SE, n=8), 35.9±3.4, and 54.6±5.0 % MVC for the 25%, 50%, and the first four contractions of the MAX exercise, respectively. Clearly, these subjects

did not on average perform as directed during the MAX exercise. Only one of the eight subjects managed to reach an average % MVC

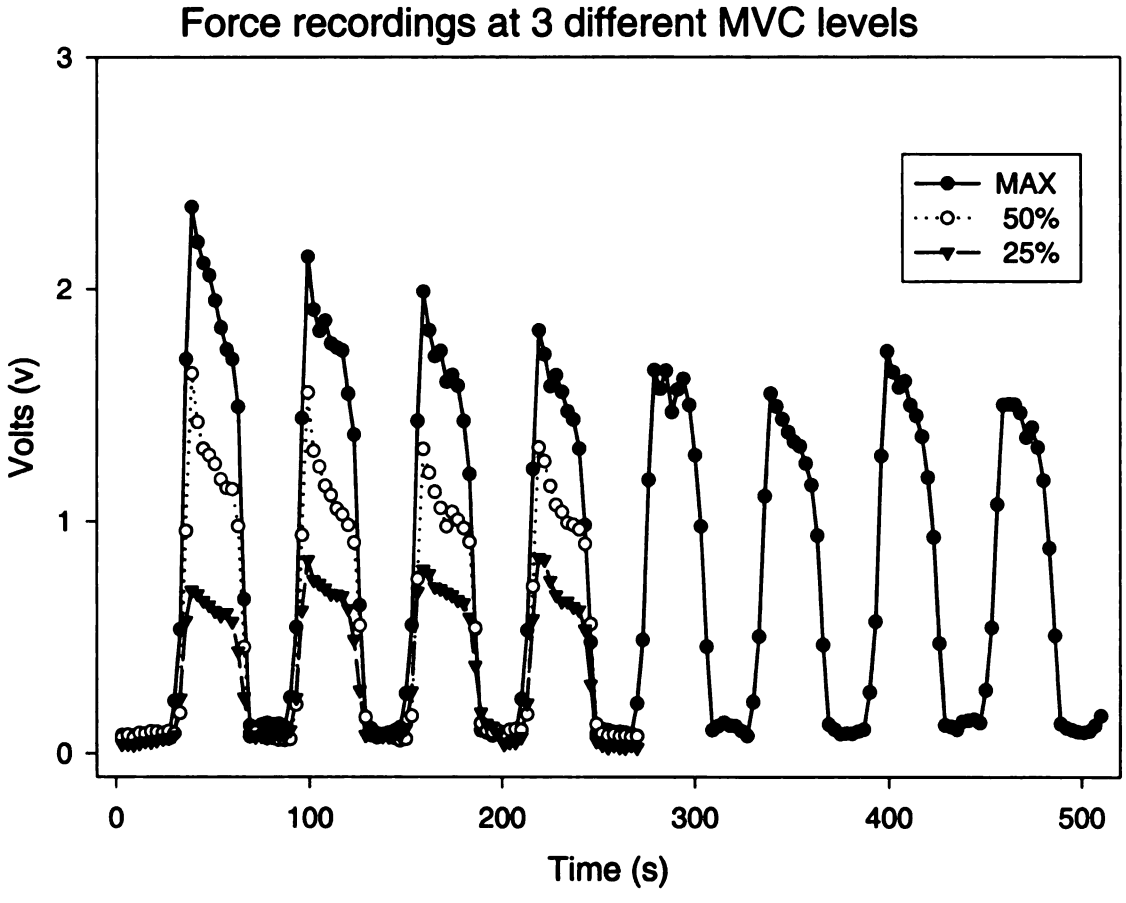

Figure 10: Raw force data recorded during the 25%, 50% and maximal MVC trials

Data from the 25,50 and MAX% MVC trials (N=8).

Table 1: Summary of raw force data

25% MVC DATA

Subject	Shift	Correlation	Rest Avg.	Average Force (v)	Reference wave	Percent MVC
1	1	0.93	0.05	0.38	1	9.05
2	0	0.77	-0.08	0.64	1	16.00
4	1	0.88	0.18	0.91	2	28.44
6	1	0.9378	0.06	0.28	1	20.00
7	0	0.95	0.1	0.17	1	15.45
10	2	0.93	0.07	0.88	1	20.95
11	0	0.912	-0.03	0.25	1	25.00
12	-1	0.94	0.07	0.55	1	24.77
AVG	(n=8)	0.913	0.07	0.53		19.89
SE		0.014	0.05	0.08		1.97

50% MVC DATA

Subject	Shift	Correlation	Rest Avg.	Average Force (v)	Reference wave	Percent MVC
1	1.00	0.94	-0.01	1.44	1	34.29
2	1.00	0.95	-0.28	1.54	1	38.50
4	1.00	0.96	0.24	1.79	1	55.94
6	1.00	0.92	0.25	0.43	1	30.71
7	1.00	0.96	0.10	0.38	1	34.55
10	1.00	0.91	0.23	0.97	1	23.10
11	1.00	0.65	0.11	0.17	1	17.00
12	1.00	0.96	0.10	0.91	1	40.99
AVG	(n=8)	0.92	0.10	1.04		35.85
SE		0.03	0.06	0.17		3.38

MAXIMAL MVC DATA

Subject	Shift	Correlation	Rest Avg.	Average Force (v)	Reference wave	Percent MVC
1	-1.00	0.96	0.05	2.55	1	60.71
2	1.00	0.94	-0.31	2.22	1	55.50
4	1.00	0.95	0.26	2.64	1	82.50
6	1.00	0.93	0.38	0.53	2	37.86
7	0.00	0.91	0.10	0.30	1	27.27
10	1.00	0.95	0.37	1.26	1	30.00
11	0.00	0.92	0.01	0.64	1	64.00
12	0.00	0.96	0.12	1.19	1	53.60
AVG	(n=8)	0.94	0.12	1.64		54.63
SE		0.00	0.07	0.32		5.04

above 70%, while 3 subjects produced an average muscle force of 40% MVC or lower during these first four cycles of the maximal MVC trial (Table 1). Similarly, the mean forces during both the "25%" and "50%" exercise were somewhat less than the target forces.

As expected, there was no substantial fatigue (i.e., decrease in mean force) over the course of the 4 contractions during the 25% and 50% exercise. There was a significant decrease in mean force between the first two vs. the last two contractions over the course of the 8 contraction MAX exercise (Figure 11, $p<0.003$). However, even in this case, the decrease ($10.9 \pm 3.9\%$) was not as great as anticipated.

Region of fMRI Activation

In the subset of eight subjects, voxels within the primary motor cortex became active with exercise in all three conditions as expected (e.g., Figure 12). Although other regions such as the ipsilateral motor areas and cerebellum were active in some subjects, this was not consistently observed in all subjects. In order to check that the alternating "REST"-"WORK" cue did not itself result in activation, fMRI data was collected in one subject who was instructed to watch the screen, but to perform no exercise. In this trial, no activation was observed in any brain region including the primary motor areas. This suggests that the observed activation during exercise is not dependent on the visual cues, holding the hand grip, magnet noise, or other incidental factors.

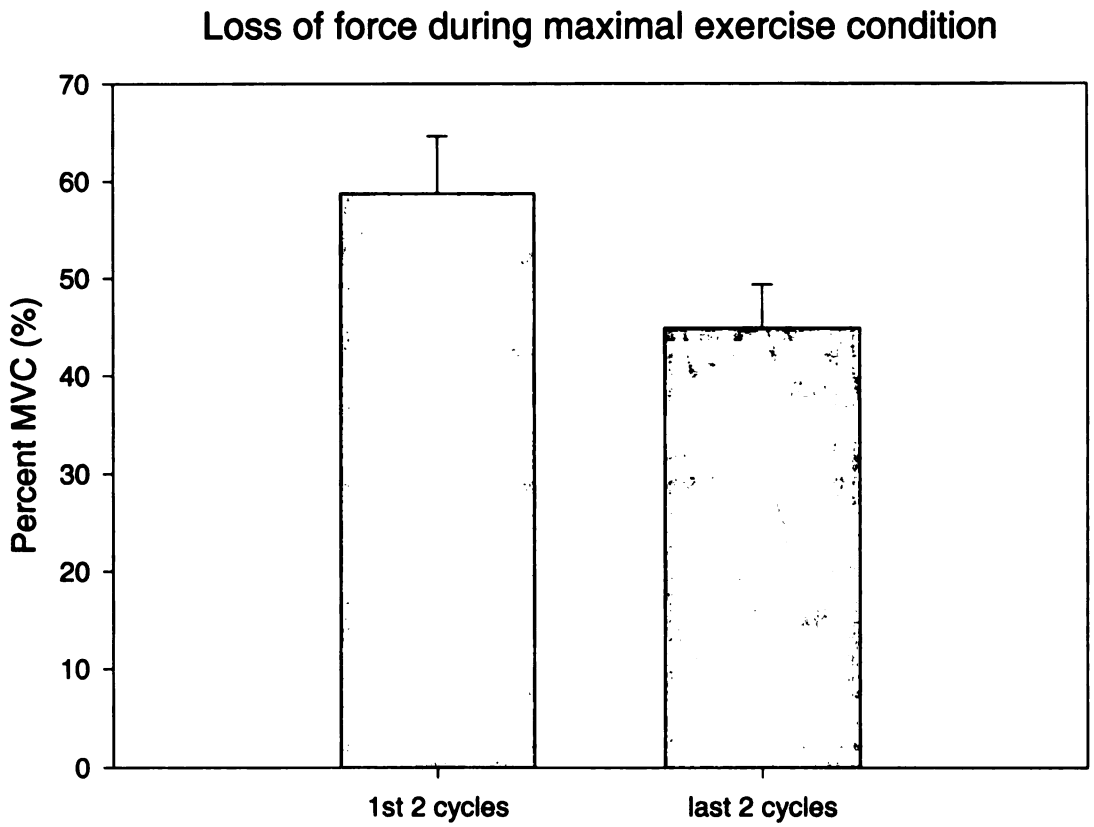

Figure 11: Loss of force from the first two cycles to the last two cycles

Average data from the 100% MVC trial (N=8) from cycles 1 and 2 were averaged and compared to the pooled data from cycles 7 and 8.

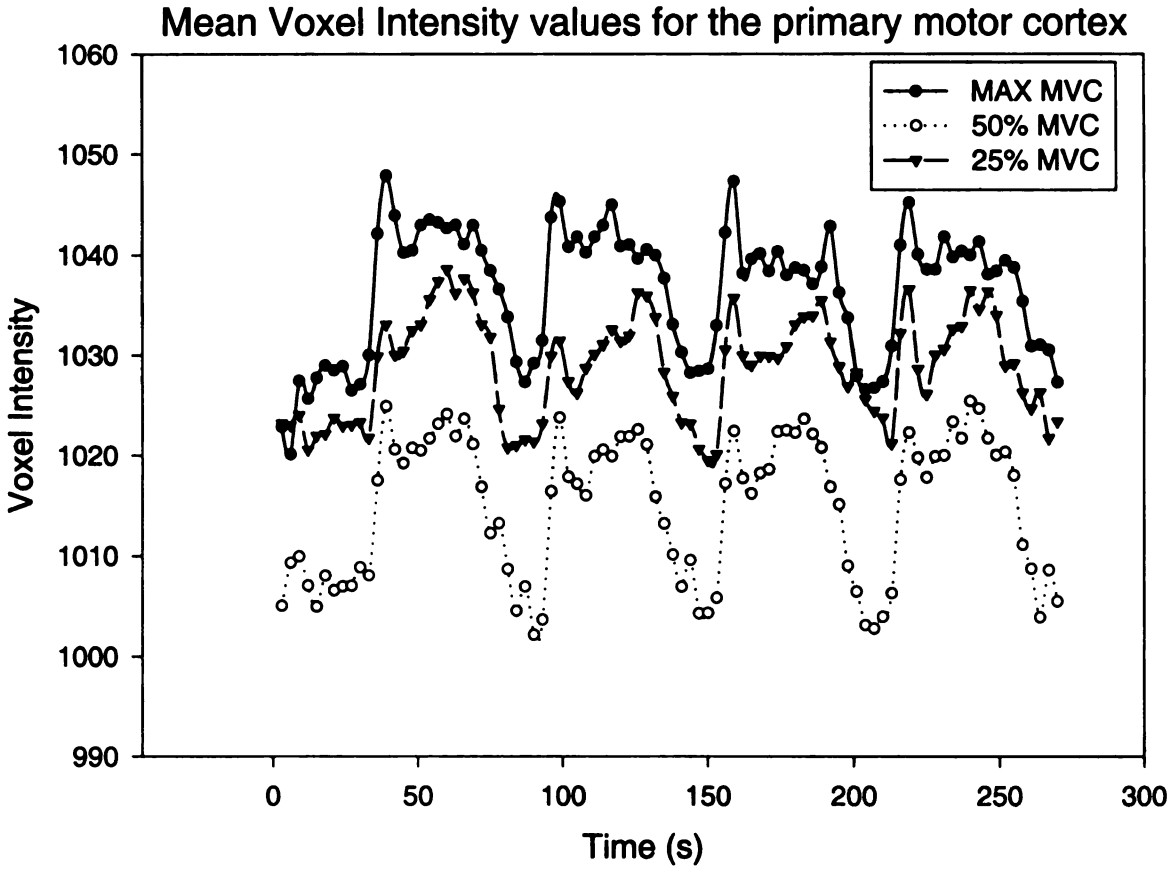

Figure 12: Signal Intensity of voxels from the primary motor area versus time for 3 different force levels

Data from MAX MVC represents the first half of the 510 second trial (N=8). The 25 and 50% trials are shown in their entirety (N=8).

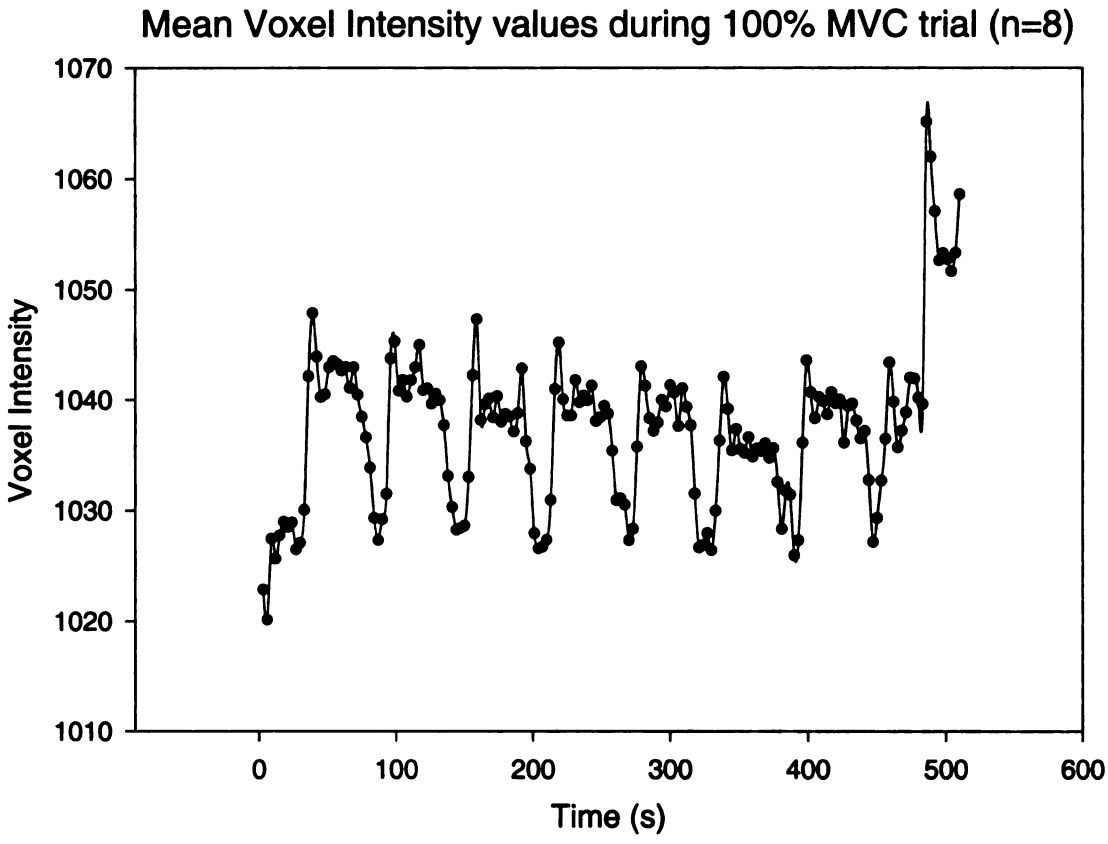

Figure 13: Mean intensity of voxels from the primary motor area versus time for 100 % MVC

Data from MAX MVC represents the full 510 second trial (N=8).

FMRI response to each of the exercise conditions

Figures 12 and 13 summarize the mean intensity from the ROI selected as described in Chapter 2 for each of the exercise conditions, and prior to motion correction. Figure 12 shows the ROI intensity for the 25%, 50% and the first half of the MAX exercise. Figure 13 shows the entire time course of the intensity variations during the MAX exercise. There was some variability in baseline intensity between the various runs. Within a trial, there was a consistent return to baseline during the rest periods. However, that return to baseline was clearly slower than the return of force to baseline (Figure 12). Presumably, this delayed recovery is due to a hemodynamic delay. As described in Chapter 2, we accounted for this effect by fitting the results to reference waves with broader on phases and shorter rest phases.

An interesting qualitative observation is the presence of a spike or peak at the onset of each of the contractions in all of the exercise conditions (figures 12 and 13). This peak appears more pronounced in the 50% and maximal MVC trials and appears to coincide with the initial peak in force. Peaks at the end of many cycles are also observed (e.g., Figure 12). All of these peaks are occurring when the hand is changing from one state to another, i.e., either from resting state to an active muscle contraction or from an active muscle contraction back to resting state.

Figures 14 and 15 show the intensity changes from the same ROI's after motion correction using the AFNI plugins. Although in some minor respects the results are modified (e.g., the drift of the last cycle in Figure 13 is corrected after motion correction), the basic results are not significantly altered.

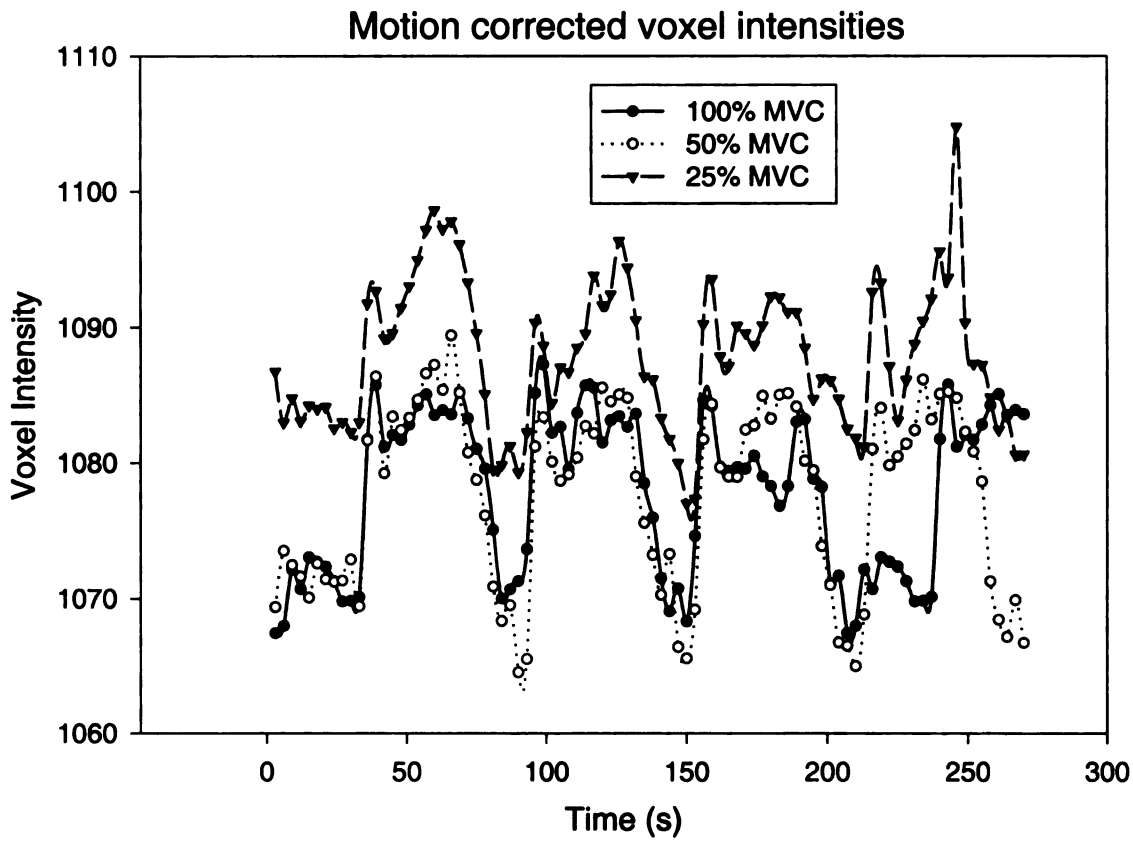

Figure 14: Motion corrected voxel intensity from the primary motor area for 3 exercise trials

Data from the 25%, 50% and Maximal MVC trials (N=8) after motion correction techniques are compared. Data from the maximal MVC trial includes only the first 270 seconds of that trial.

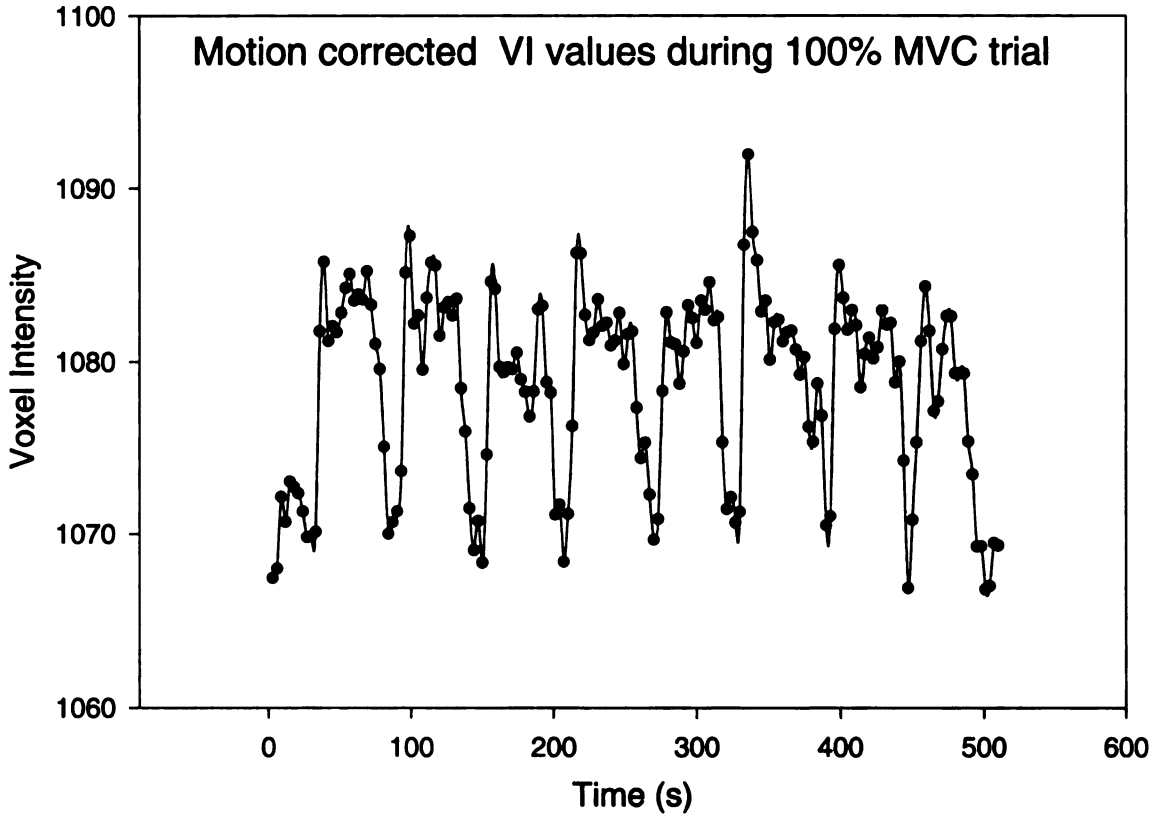

Figure 15: Motion corrected signal intensity of voxels from the primary motor area during the maximal MVC trial

Data from the 100% MVC trial (N=8) after motion correction techniques were applied. The abnormally high peaks occurring in figure 13 have been corrected. Eight distinct cycles of signal activation are visible.

Table 2: Summary of raw voxel intensity data

25% RAW VOXEL INTENSITY DATA

Subject	Shift	Correlation	Rest Avg.	Intensity increase	Reference wave	Percent Change
1	1	0.88	1058	17.2	4	1.628
2	1	0.75	840	17.9	6	2.1
4	5	0.54	1030	9.48	2	0.92
6	1	0.53	1175	4.9	5	0.41
7	1	0.64	1132	5	5	0.44
10	1	0.57	932	9.6	5	1.03
11	2	0.39	1064	5.23	7	0.491
12	1	0.83	946	12.07	4	1.27
AVG	(n=8)	0.64	1022	10.17		1.04
SE		0.0591	39.10	1.85		0.21

50% - RAW VOXEL INTENSITY

Subject	Shift	Correlation	Rest Avg.	Intensity increase	Reference wave	Percent Change
1	1	0.86	1070.00	18.20	4	1.70
2	1	0.88	849.00	26.00	5	3.10
4	1	0.82	1033.00	17.70	5	1.70
6	1	0.80	1161.00	8.70	4	0.75
7	1	0.71	1089.00	8.50	4	0.78
10	1	0.79	926.00	16.40	6	1.77
11	2	0.38	1036.00	5.59	3	0.54
12	0	0.75	881.00	14.55	3	1.65
AVG	(n=8)	0.75	1005.63	14.46		1.50
SE		0.06	38.57	2.35		0.29

100% - RAW VOXEL INTENSITY

Subject	Shift	Correlation	Rest Avg.	Intensity increase	Reference wave	Percent Change
1	0	0.59	1032.00	15.50	3	1.50
2	-7	0.70	855.00	24.00	2	2.80
4	1	0.85	1033.00	16.60	5	1.60
6	1	0.74	1188.00	9.90	4	0.83
7	1	0.66	1142.00	9.50	7	0.83
10	1	0.86	925.00	23.10	5	2.49
11	1	0.67	1114.00	14.10	6	1.27
12	1	0.84	921.00	23.40	4	2.60
AVG	(n=8)	0.74	1026.25	17.01		1.74
SE		0.04	41.83	2.09		0.28

Table 3: **Summary of motion corrected voxel intensity data**

25% - MOTION CORRECTED VOXEL INTENSITY

Subject	Shift	Correlation	Rest Avg.	Intensity increase	Reference wave	Percent Change
1	1	0.85	1132	15.7	4	1.38
2	1	0.73	916	14.5	4	1.58
4	5	0.6	1013	15.01	1	1.48
6	0	0.17	1336	1.28	6	0.1
7	1	0.57	1156	7.52	4	0.65
10	7	0.48	947	11.89	1	1.26
11	7	0.37	1151	5.86	1	0.51
12	1	0.55	1008	10.64	2	1.06
AVG	(n=8)	0.54	1082	10.30		1.00
SE		0.0739	48.78	1.79		0.187

50% - MOTION CORRECTED VOXEL INTENSITY

Subject	Shift	Correlation	Rest Avg.	Intensity increase	Reference wave	Percent Change
1	1	0.87	1142	18.46	3	1.62
2	1	0.89	926	20.41	4	2.2
4	1	0.84	1048	27.8	6	2.65
6	-7	0.23	1294	2.53	1	0.2
7	1	0.77	1164	13.84	3	1.19
10	6	0.75	971	17.68	1	1.82
11	6	0.19	1030	3.07	1	0.3
12	0	0.75	977	13	4	1.34
AVG	(n=8)	0.66	1069	14.599		1.42
SE		0.10	43.39	3.03		0.30

100% - MOTION CORRECTED VOXEL INTENSITY

Subject	Shift	Correlation	Rest Avg.	Intensity increase	Reference wave	Percent Change
1	0	0.78	1124	17.68	3	1.57
2	-7	0.73	926	20.30	2	2.19
4	1	0.89	1014	29.30	5	2.89
6	7	0.48	1286	7.10	2	0.55
7	1	0.59	1108	6.52	4	0.59
10	1	0.78	945	22.72	6	2.40
11	4	0.37	1146	7.16	3	0.62
12	1	0.73	1002	16.43	4	1.64
AVG	(n=8)	0.67	1068.88	15.90		1.56
SE		0.06	42.45	2.96		0.32

The detailed results of the ROI vs. reference wave correlation analysis are summarized in Tables 2 (before motion correction) and 3 (after motion correction). The column labeled "Shift" in the Tables represents the number of points that the reference was shifted in order to obtain the best fit with the fMRI data. Positive numbers reflect shifts to the right, while negative numbers reflect shifts to the left. Figure 9 for example, has a rightward shift of 1, corresponding to a delay of 3 seconds. The fact that in almost all cases the shift was positive is consistent with the expected hemodynamic delay between neural activity and the BOLD response. The "wave" in the Tables refers to which of the 7 reference waves (Figure 8) gave the best fit. The fact that in most cases the broader on-phase references gave the best fit confirms the qualitative impression that the hemodynamic response persisted into the rest periods.

There was as significant increase in the percent change in ROI intensity for the 50% and the first 4 contractions of the MAX exercise compared to the 25% exercise ($p<0.025$ for 50% vs. 25%, paired t-test; $p<0.007$ for MAX vs. 25%). This conclusion was essentially unaltered by the motion correction (Figure 16). However, the MAX trial did not statistically differ from the 50% MVC trial ($P > 0.15$ for both non-motion corrected and motion corrected data). The variance within each of the groups was not equal using the Levine test of homogeneity of variance ($P < 0.05$). The unequal variance is not too great a concern as the crucial test is the paired comparison between exercises.

Figure 17 shows the relationship between the ROI intensity changes and the force developed during the first four contractions of the three exercises for the individual subjects. The lines are simple linear regressions for each subject. Because the variations in both force and ROI intensity varied widely between different subjects, a simple

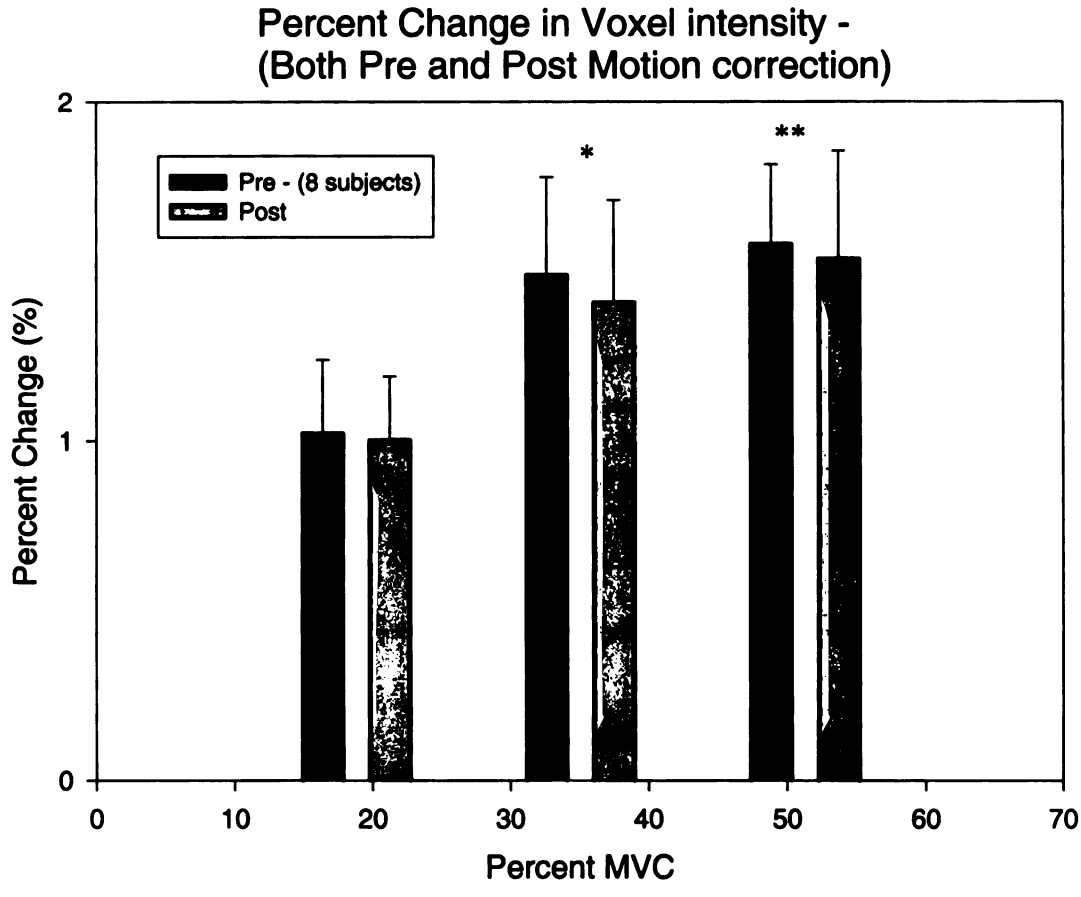

Figure 16: Bar graph showing percent change in voxel intensity in raw and motion corrected data

Black bars represent pre motion corrected data. Grey bars represent motion-corrected data. * $p<0.025$ for 50% vs. 25%, ** $p<0.007$ for MAX vs. 25%. No difference exists between pre motion correction data and post motion corrected data.

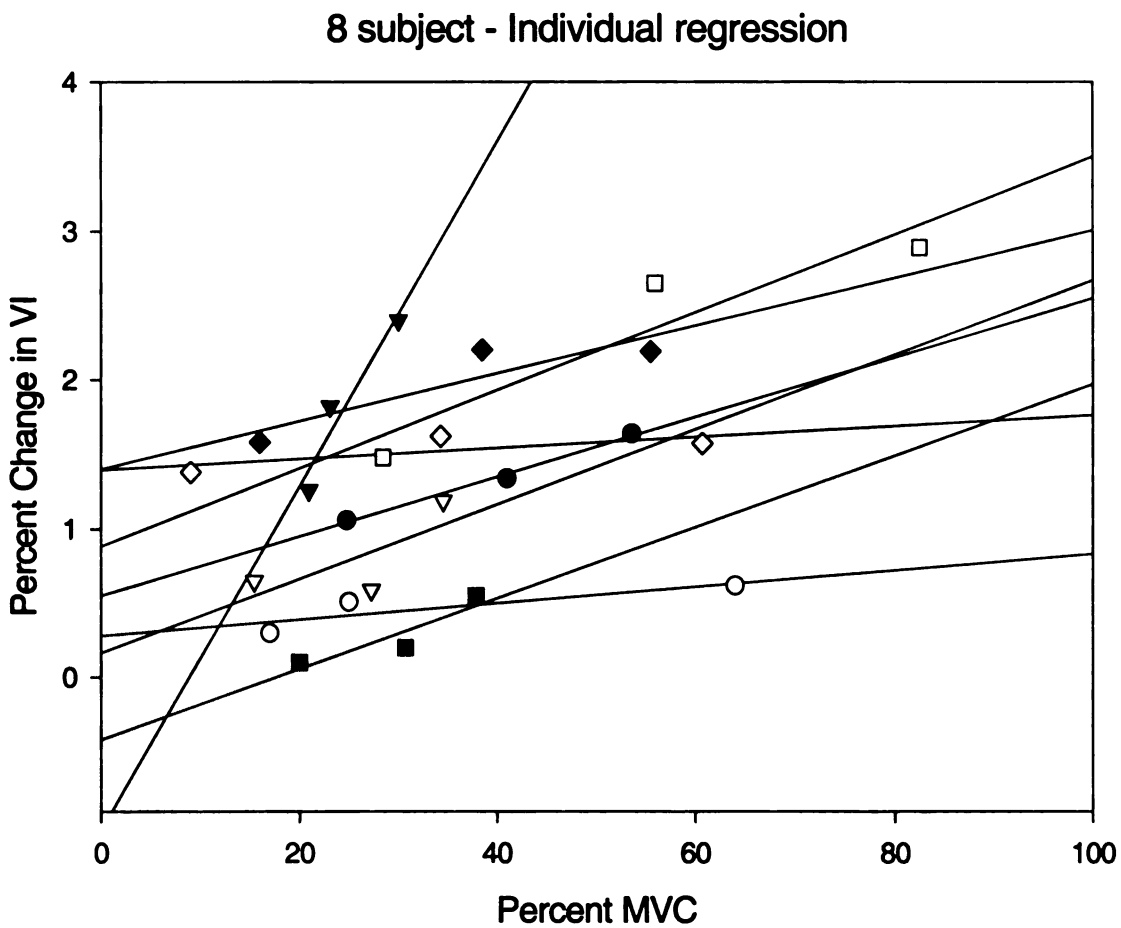

Figure 17: Simple linear regressions of individual subjects

Each individual correlation shows an upward trend as the relative force level increases so too does the percent change in voxel intensity.

regression of data from all the subjects was not significant. While there is a general trend for increased fMRI response with increased force, this trend may be obscured by the fact that the force during the MAX exercise was not greatly different than during the 50% exercise.

Effects of fatigue on signal intensity

In order to induce muscle fatigue, the maximal MVC trial was twice as long as the other two trials. However, as discussed above, the decrease in force during this exercise was only ($10.9 \pm 3.9\%$, $p<0.003$, see Figure 11). Figure 18 shows the ROI intensity changes during the first two contractions vs. the last two contractions of the MAX exercise. No significant difference in signal intensity was observed for either the non-motion corrected time series ($P> 0.05$) and the motion corrected time series ($P>0.05$). The non-motion corrected time series showed a high degree of variability between subjects and was noticeably reduced by motion correction. In any case, neither analysis provides evidence that the fMRI response was altered by fatigue.

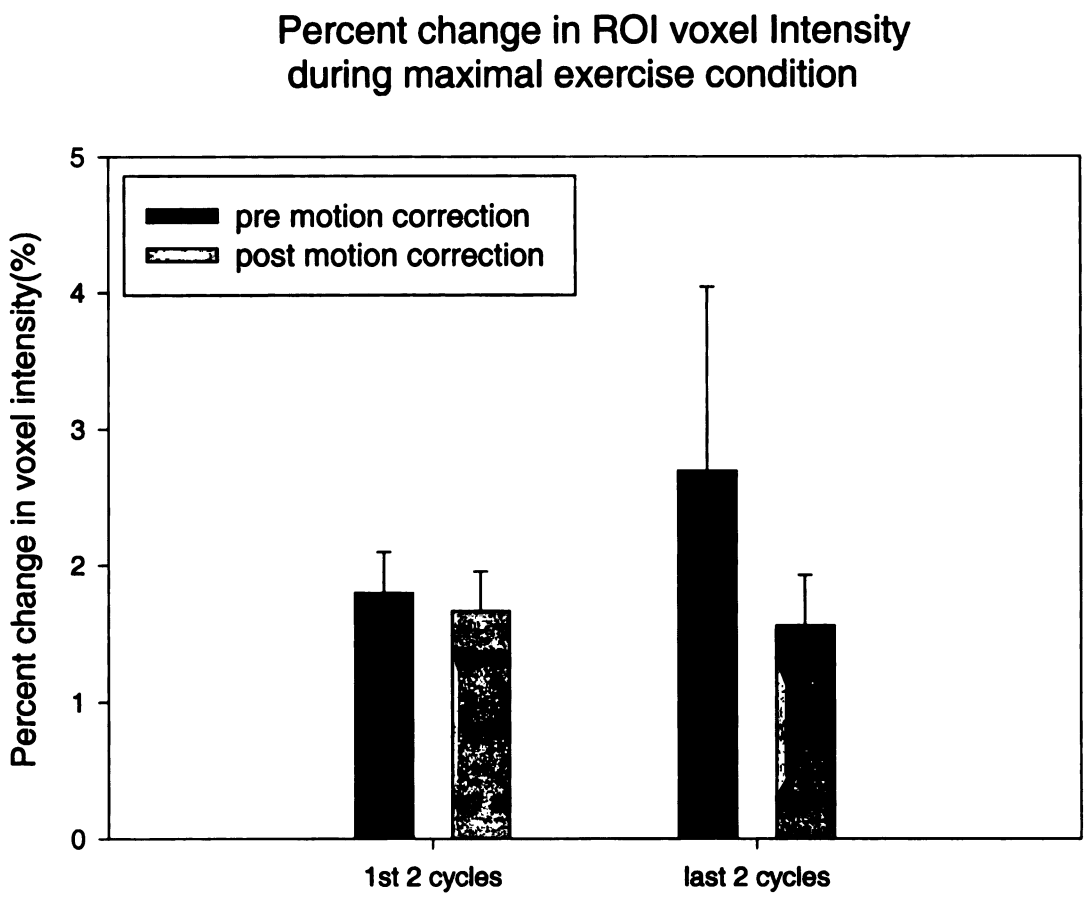

Figure 18: Comparison of first 2 cycles to the last 2 cycles of the raw and motion corrected voxel intensity data

There is no significant difference between the first 2 cycles and the final 2 cycles in either the pre motion corrected or motion corrected data.

Chapter 4: Discussion and Future Directions

The main results of this study are, first, that increased force of isometric muscle contraction is associated with increased intensity of the BOLD response in the motor cortex, and second, that muscle fatigue is not accompanied by a significant change in the BOLD response during isometric contraction.

The first aim of the study involved varying levels of muscle force to determine if this would have an effect on the intensity of the BOLD response in the primary motor cortex. We found an increase in ROI intensity which was significant between 25% MVC and 50% or "MAX" conditions. There was no significant difference between the 50% and MAX conditions, but this result may simply reflect the fact that our subjects did not actually develop their maximum MVC during that trial. Because our data only extends from about 20% to 55 % of MVC (e.g, Figure 16), we have not fully characterized the dependence of the fMRI response on force. However, based on our results over this limited range, it appears that the relationship between isometric force and fMRI response is not linear. There are at least two possible explanations for the apparent non-linear response. First, it may be that the neural activity of the ROI is accurately measured by fMRI, and that activity is not linear with force. For example, it could be that only a fraction of the neurons in the ROI are involved in force generation, and that the ROI includes other neurons which are involved in such things as initiation of force, feedback regulation, regulation of the rate of force development and relaxation, etc. The activity of these other neurons may not depend on the absolute force developed during the

maintained contractions. Second, it may be that the fMRI response is not an accurate measure of the average neuron activity in the ROI. For example, the BOLD response may approach saturation at less than the maximum force generation. Alternatively, it may be that metabolism in the glial cells contributes a substantial component to the BOLD effect, and that glial metabolism is not proportional to the underlying neural activity.

Although the relationship was not linear, this is the first study to report a significant increase in BOLD intensity vs. force of muscle contraction. These findings are not consistent with the earlier results of Ludman et al., who reported no effect of force on fMRI response during a dynamic weight-lifting exercise (Ludman et al. 1996). However, it should be noted that the intensity of the motor cortex response reported in Ludman et al. was 2-5%, whereas the greatest mean change observed in this study was less than 2%. Therefore, the overall response to dynamic contractions is clearly greater than to isometric contractions. This difference between dynamic vs. isometric contractions was previously reported by Thickbroom et al. (Thickbroom et al. 1999). In fact, in their first paper, Thickbroom et al. did report a trend toward increased response with increased force during isometric contractions, but the trend did not reach statistical significance (Thickbroom et al. 1998).

The second aim of this study was to examine if fatigue is accompanied by a significant change in the intensity of the response in the activated region of the motor cortex. We found no significant difference between the intensity of the response near the start vs. near the end of the MAX exercise (Figure 18). However, the extent of fatigue in this study was not dramatic, largely because the subjects did not begin contracting at their measured MVC. Therefore, the failure to observe any change in the fMRI response is not

conclusive. It does appear that the marginal fatigue observed in this study is not accompanied by a measurable change in fMRI response. Therefore, based on this limited result, there is no evidence for a "central component" in the fatigue. Of course, the failure to detect a change in response with fatigue in this experiment does not mean it could not be observed under different conditions. In fact, our protocol may not be ideal for causing central fatigue. As mentioned in Chapter One, central fatigue is thought to be more important at low levels of force (20-25%) over a longer duration of muscle contraction (20 minutes or more, vs. 8.5 min in this study). Unfortunately, a study of long duration exercise would raise many other technical problems, for example, increased chance of motion artifacts and instrumentation errors.

It may be that presenting the subjects with visual feedback of their force would have improved subject compliance during the MAX exercise, and resulted in greater fatigue during that exercise. For example, in the studies by Thickbroom et al., subjects could see the force developed on a sphygmomanometer. However, we chose not to display the force record to the subjects during the experiments for two reasons. First, in our early pilot studies, we did allow visual feedback during the exercise trials. This allowed for maintenance of the target force level, but subjects tended to neglect the need to prevent head motion, especially at the higher forces. Subjects demonstrated accuracy at each of the lower levels of force, i.e., levels below 60% MVC. However, at higher forces, the subjects began to use arm and shoulder muscles in order to achieve the target force. This always resulted in some sort of head motion, and excessive motion artifacts in the functional images. Second, as discussed in Chapter 1, we were concerned that the

feedback would involve an additional cognitive activity, which might obscure activity dependent on the force per se.

Despite our efforts to limit head motion, motion artifacts were still a problem in this study, and resulted in rejection of data from three of the subjects. A number of techniques have been used to reduce head motion, including clamping the head in place to restrict movement and the use of bite bars. Head clamping hasn't been successful for longer scans as pressure points on the head cause discomfort and subject motion (Zeffiro 1996). Bite bars can be successful for reducing head motion but are uncomfortable, and anecdotal reports suggest they increase the sensation of claustrophobia in the magnet. Because our subjects volunteered without any compensation, the use of the bite bar was rejected for this study. Another strategy to prevent head motion involves behavioral feedback. This involves training the subject to remain motionless during scans and is effective in reducing head motion (Zeffiro 1996). Unfortunately, in this experiment extensive training was not practical, again, because the subjects were asked to volunteer without any compensation.

In addition to the main results, we observe spikes in the intensity of the ROI at the beginning and end of the "on" cycles of the exercise. These spikes coincided with an active effort from the subject to either generate muscle force or to relax the hand. This suggests that changing from one static level of muscle activation to another require an increase in neural activity in the selected ROI (Toma et al. 1999). The observed spikes could be related to the more robust fMRI response that occurs during dynamic exercise (Thickbroom et al., 1999). Even though our isometric handgrip exercise did not allow any joint flexion, a sensory and proprioceptive component is present and could be

enhanced at the beginning and ending of the contractions. At the onset of an isometric contraction, some shortening of the muscle fibers must occur and as muscle tension rises, sensory receptors will be activated in the muscles, tendons and in the joints of the hand. This milieu of sensory feedback likely isn't as pronounced as in a dynamic exercise, but could still be sufficient to cause the spikes.

Based on the experience gained in this study, future studies could be improved in some respects. For example, it would be helpful to have subjects practice the entire protocol out of the magnet prior to the actual imaging. In practice sessions, visual feedback would be included so that the subjects would be aware of the tendency to decrease force over the course of the 30 s contractions. Practice would also provide an opportunity for the investigator to coach the subjects not to recruit neck and shoulder muscles during the exercise, and to remind subjects to lie still during the rest periods. Finally, subjects could be better trained in the use of the handgrip device during practice sessions. This is important, because if the subject repositions his/her hand during the experiment, the lever arm of the device changes, and the effective MVC can change. The practice would have to be held on separate days from the actual fMRI sessions to allow for recovery from muscle fatigue. A 2-3 day commitment from subjects would likely be necessary. Development of a more comfortable handgrip would also be worthwhile. Some subjects, especially those with smaller hands, found the grip to be slippery, and had difficulty maintaining a secure grip. A device that fixed the hand into position, for example a glove-like device, would be an improvement.

Another improvement would be to acquire sagital slices during the fMRI acquisitions rather than axial slices. The most severe motion artifacts encountered in this

study appeared to be due to movement along the superior-inferior axis, rather than to rotation or translation in the axial plane. Because we used axial slices, the spatial resolution in this study is lowest in the superior-inferior direction, making motion correction more difficult in this direction. Although the motion correction algorithms did improve the quality of the data, particularly near the end of the MAX exercise, these algorithms could not rescue three of the 13 data sets.

A logical continuation of this study would be to repeat the same basic protocol, but switch from one force level to another force level rather than returning to rest during each cycle (e.g., using 25% MVC as the resting state and 50% MVC as the active state). This would check both the specificity of the intensity changes to force level, and also enable exploration of the cause of the spikes observed at the onset and end of the contractions. Another useful variation would be to simply instruct the subjects to change the force at regular intervals, but give no detailed pattern of target forces. In such a protocol, the force record (appropriately shifted as necessary) could be used as the reference wave for cross-correlation statistics.

In summary, there were two major findings of this study. First, the results show that there is a significant effect of isometric force on the fMRI response in the contralateral motor cortex. Second, the results provide no evidence that the fMRI response in the motor cortex is altered by muscle fatigue. However, further studies will be needed to demonstrate the generality of these results to other exercise and fatigue conditions.

References

Adams, G.R., M.J. Fisher, R.A. Meyer. (1991) Hypercapnic acidosis and increased $H_2PO_4^-$ concentration do not decrease force in cat skeletal muscle. *Am J Physiol* **260**(4 pt 1):C805-12.

Bandettini, P. A., E. C. Wong, et al. (1992). "Time course EPI of human brain function during task activation." Magn Reson Med **25**(2): 390-7.

Belanger, A. Y. and A. J. McComas (1981). Extent of motor unit activation during effort: *J Appl Physiol* 1131-1135.

Bellemare, F., F. Furbrush, B. Bigland-Ritchie (1984). Localization of human diaphragm fatigue. *Fed prod Abst,* **42:**530, 1984.

Bigland-Ritchie, B. and J. J. Woods (1984). Changes in muscle contractile properties and neural control during human muscular fatigue: *Muscle Nerve* 691-699.

Bigland-Ritchie, B., F. Furbush and J. J. Woods (1986). Fatigue of intermittent submaximal voluntary contractions: central and peripheral factors: *Journal of Applied Physiology* **61:**421-429.

Blamire, A. M., S. Ogawa, et al. (1992). Dynamic mapping of the human visual cortex by high-speed magnetic resonance imaging. *Proc Natl Acad Sci U S A* **89**(22): 11069-73.

Boroojerdi, B., H. Foltys, et al. (1999). "Localization of the motor hand area using transcranial magnetic stimulation and functional magnetic resonance imaging." Clin Neurophysiol 110(4): 699-704.

Brust, J. (1991). Cerebral circulation: Stroke. **Principles of Neural Science**. E. Kandel, J.H. Schwartz, T.M. Jessel. New York, Appleton and Lange: 1041-1049.

Cady, E.B., D.A. Jones, J. Lynn, D.J. Newham, (1989). Changes in force and intracellular metabolites during fatigue of human skeletal muscle. *J Physiol,* **418:** 311-25.

Chen, R. (2000). "Studies of human motor physiology with transcranial magnetic stimulation." *Muscle Nerve* **999**(9): S26-S32.

Cote L., M. D. C. (1991). The Basal Ganglia, chapter 42. **Principles of Neural Science, 3rd Ed.** J. H. S. E.R. Kandel, T.M. Jessel (eds). New York, Appleton and Lange: 647-654.

Cox, R. W. (1996). AFNI: software for analysis and visualization of functional magnetic resonance neuroimages: *Computers and Biomedical research,* 162-173.

Deecke, L., P. Scheid, et al. (1969). "Distribution of readiness potential, pre-motion positivity, and motor potential of the human cerebral cortex preceding voluntary finger movements." *Exp Brain Res* **7**(2): 158-68.

Dettmers C., G.R. Fink, R.N. Lemon, K.M. Stephan. R.E. Passingham, D. Silbersweig, A. Holmes, M.C. Ridding, D.J. Brooks, R.S.J. Frackowiak (1995). Relation between cerebral activity and force in the motor areas of the human brain. *J Neurophysiol,* **74:**802-815.

Ellerman J, M. G., K Hendrich, R Hinke, X Hu, SG Kim, R Menon, H Merkle, S Ogawa, K Ugurbil (1994). Functional imaging of the brain by nuclear magnetic resonance. NMR in Pjusiology and Biomedicine. G. RJ. New York, Academic Press: 137-150.

Enoka, R. M. and D. G. Stuart (1992). Neurobiology of muscle fatigue: *J Appl Physiol* 1631-1648.

Enoka, R.M., (1996) Eccentric contractions require unique activation strategies by the nervous system. *J Appl Physiol*, **81**(6): 2339-46.

Farrar, T., DE Becker (1971). Pulse and Fourier Transform NMR. New York, Academic Press.

Fitts, R.H. (1994). Cellular mechanisms of muscle fatigue. *Physiological Reviews,* **74**(1):49-94.

Fox, P.T., M.A. Mintun, M.E. Raichle, F.M. Miezin, J.M. Allman, D.C. Van Essen. (1986) Mapping human visual cortex with positron emission tomography. *Narure,* **323**(6091):806-9.

Ganong, W. (1991). Ciculation through special regions. Review of Medical Physiology, 15th ed. Norwalk, CT, Appleton and Lange: 570-572.

Ghez, C. (1991). The cerecellum. **Principles of Neural Science, 3rd Ed.,**. J. H. S. Kandel, T.M. Jessel (eds). New York, Appleton and Lange: 618-641.

Grubb, R. L., Jr., M. E. Raichle, et al. (1974). "The effects of changes in PaCO2 on cerebral blood volume, blood flow, and vascular mean transit time." *Stroke* **5**(5): 630-9.

Gyngell, M. L., C. Bock, et al. (1996). "Variation of functional MRI signal in response to frequency of somatosensory stimulation in alpha-chloralose anesthetized rats." *Magn Reson Med* **36**(1): 13-5.

Hales, J. P. and S. C. Gandevia (1988). Assessment of maximal voluntary contraction with twitch interpolation: an instrument to measure twitch responses: ***J Neurosci methods*** 97-102.

Hornak, J. P. (2000). The basics of MRI. http://www.cis.rit.edu/htbooks/mri/inside.htm. **2000**.

Ilmoniemi, R. J., J. Ruohonen, et al. (1999). "Transcranial magnetic stimulation--a new tool for functional imaging of the brain." *Crit Rev Biomed Eng* **27**(3-5): 241-84.

Kandel ER, S. S., Schwartz JH. (1991). Synaptic Transmission. **Principles of Neural Science, 3rd Ed.** J. H. S. E.R. Kandel, T.M. Jessel. New York, Appleton and Lange: 123-134.

Kelly, J. P. (1991). The neural basis of perception and movement. **Principles of Neural Science, 3rd Ed.** J. H. S. E.R. Kandel, T.M. Jessel (eds). New York, Appleton and Lange: 293-295.

Koechlin, E., G. Corrado, et al. (2000). "Dissociating the role of the medial and lateral anterior prefrontal cortex in human planning." *Proc Natl Acad Sci U S A* **97**(13): 7651-6.

Lim, S. H., D. S. Dinner, et al. (1994). "Functional anatomy of the human supplementary sensorimotor area: results of extraoperative electrical stimulation." *Electroencephalogr Clin Neurophysiol* **91**(3): 179-93.

Ludman, C. N., T. G. Cooper, et al. (1996). "Force of voluntary exercise does not affect sensorimotor cortex activation as detected by functional MRI at 1.5 T." *NMR Biomed* **9**(5): 228-32.

Martin, J. H., J.C. Brust, S. Hilal (1991). Imaging the Living Brain. **Principles of Neural Science, 3rd Ed**. E. R. Kandel, J.H. Schwartz, T.M. Jessel. New York, Appleton and Lange: 309-324.

McKenzie, D.K., B. Bigland-Ritchie, R.B. Gorman, S.C. Gandevia. (1992). Central and peripheral fatigue of human diaphragm and limb muscles assessed by twitch interpolation. *J Physiol,* **454:**167-76.

Merton, P. A. (1954) Voluntary strength and fatigue, *J. Physiol. London,* **123**:553-564.

Merton, P. A. and H. B. Morton (1980). "Stimulation of the cerebral cortex in the intact human subject." *Nature* **285**(5762): 227.

Ogawa, S., T. M. Lee, et al. (1990). Brain magnetic resonance imaging with contrast dependent on blood oxygenation: ***Proc Natl Acad Sci*** 9868-9872.

Ogawa, S., R. S. Menon, et al. (1998). "On the characteristics of functional magnetic resonance imaging of the brain." *Annu Rev Biophys Biomol Struct* **27**: 447-74.

Ogawa, S., R. S. Menon, et al. (1993). "Functional brain mapping by blood oxygenation level-dependent contrast magnetic resonance imaging. A comparison of signal characteristics with a biophysical model." Biophys J 64(3): 803-12.

Olesen, J. (1971). "Contralateral focal increase of cerebral blood flow in man during arm work." *Brain* **94**(4): 635-46.

Porter, R. J. W. (1981). Human Muscle fatigue: physiological mechanisms. London, Pitman Medical.

Raichle, M. E., R. L. Grubb, Jr., et al. (1976). "Correlation between regional cerebral blood flow and oxidative metabolism. In vivo studies in man." *Arch Neurol* **33**(8): 523-6.

Ramsey, N. F., B. S. Kirkby, et al. (1996). "Functional mapping of human sensorimotor cortex with 3D BOLD fMRI correlates highly with H2(15)O PET rCBF." *J Cereb Blood Flow Metab* **16**(5): 755-64.

Rao, S.M., J.R. Binder, P.A. Bandettini, T.A. Hammeke, F.Z. Yetkin, A. Jesmanowicz, L.M. Lisk, G.L. Morris, W.M. Mueller, L.D. Estkowski, E.C. Wong, V.M. Haughton, J.S. Hyde. (1993) Functional magnetic resonance imaging of complex human movements. *Neurology,* 43, 2311-2318

Rapoport, S. I. (1976). Bllod-Brain Barrier in Physiology and Medicine. New York, Paven Press.

Roberts, T. P. and H. A. Rowley (1997). "Mapping of the sensorimotor cortex: functional MR and magnetic source imaging." AJNR Am J Neuroradiol 18(5): 871-80.

Roland, E. and B. Larsen (1976). "Focal increase of cerebral blood flow during stereognostic testing in man." *Arch Neurol* **33**(8): 551-8.

Roland, P. E., B. Larsen, et al. (1980). "Supplementary motor area and other cortical areas in organization of voluntary movements in man." *J Neurophysiol* **43**(1): 118-36.

Rothwell, J. C. (1997). "Techniques and mechanisms of action of transcranial stimulation of the human motor cortex." *J Neurosci Methods* **74**(2): 113-22.

Savoy, R.L. (2001) History and future directions of human brain mapping and functional neuroimaging. *Acta Psychol,* **107**(1-3):9-42.

Schwartz, J., Ed. (1991). Synaptic Vesicles. **Principles of Neural Science, 3rd Ed.**, New York, Appleton and Lange.

Shaw, D. (1976). Relaxation. Fourier Transform N.M.R. Spectroscopy. S. D. New York, Elsevier Scientific Publishing Company: 297-298.

Schleicher A, A. K., Geyer S, Kowalski T, Schormann T, Palomero-Gallagher N, Zilles K (2000). "A stereological approach to human cortical architecture: identification and delineation of cortical areas." *J Chem Neuroanat* **20**(1): 30-47.

Thickbroom, G., B. A. Phillips, et al. (1998). Isometric force-related activity in sensorimotor cortex measured with functional MRI: ***Exp Brain Res,* 121**:59-64.

Thickbroom, G. W., B. A. Phillips, et al. (1999). "Differences in functional magnetic resonance imaging of sensorimotor cortex during static and dynamic finger flexion." Exp Brain Res 126(3): 431-8.

Thickbroom, G. W., M. L. Byrnes, et al. (2000). "The role of the supplementary motor area in externally timed movement: the influence of predictability of movement timing." *Brain Res* **874**(2): 233-241.

Thulborn, K. R. (1999). Visual feedback to stabilize head position for fMRI**:** 1039-1043. Yoshizawa, T., T. Nose, et al. (1996). "Functional magnetic resonance imaging of motor activation in the human cervical spinal cord." *Neuroimage* **4**(3 Pt 1): 174-82.

Toma, K., M. Honda, T. Hanakawa, T. Okada, H. Fukuyama, A. Ikeda, S. Nishizawa, J. Konishi, H. Shibasaki. (1999) Activities of the primary and supplementary motor areas increase in preparation and execution of voluntary muscle relaxation: An event-related fMRI study. *J Neurosci,* **19(9):** 3527-34.

Yetkin, F. Z., W. M. Mueller, et al. (1995). "Functional magnetic resonance imaging mapping of the sensorimotor cortex with tactile stimulation." Neurosurgery 36(5): 921-5.

Zeffiro, T. (1996) Clinical functional image analysis: artifact detection and reduction. *Neuroimage,* **4(3 pt 3)**: S95-100.